NASA
DIRECTOR OF LOGISTICS OPERATIONS
MATERIALS SCIENCE DIVISION
MATERIALS AND CHEMICAL ANALYSIS BRANCH
LO-MSD-1M
KENNEDY SPACE CENTER, FLORIDA 32899

APRIL 17, 1995

94-2082

SUBJECT: Evaluation of Inorganic Zinc-Rich Primers (ZRP's) Using Electrochemical Impedance Spectroscopy (EIS) in Combination With Atmospheric Exposure.

RELATEDDOCUMENTATION: KSC-STD-C-0001
DM-MSL Report MTB 268-86B
DM-MSL Report MTB 268-86C
DM-MSL Report MTB 610-89A
DM-MSL Report 91-4336
DM-MSL Report 91-4821
DM-MSL Report 93-2004

1.0 SUMMARY

This investigation explored the use of EIS in combination with atmospheric exposure at the Kennedy Space Center (KSC) Beach Corrosion Test Site near the Space Shuttle launch complex as a short-term method for analyzing the performance of 21 commercially available ZRP's. EIS measurements were collected after different times of atmospheric exposure and analyzed by finding an equivalent circuit to simulate the data. This analysis yielded several parameters indicative of physical and chemical behavior for the new and aged primer films. These parameters were analyzed and summarized to help categorize the behavior of each material. A correlation was found between the long-term performance of ZRP's and several parameters from the EIS measurements; work will continue to refine the evaluation process and improve the prediction capabii of this technique.

2.0 FOREWORD

2.1 For over 25 years, the process of coating testing at KSC to identify materials for the long-term protection of carbon steel structures has taken place at the Beach Corrosion Test Site near the Space Shuttle launch complex. The atmosphere at the launch pad is highly corrosive due to the proximity of the ocean, heat from rocket exhaust, and now with the Space Shuttle, the acidic combustion products from the Solid Rocket Boosters (SRB's). As a result of previous long-term

exposure tests, ZRP's were identified as the best choice to provide long-term protection of launch structures and ground support equipment at KSC.

2.2 Exposure at the beach site provides very valuable data, but it takes a long time. Testing requires 18 months for prehminary approval, and continued good performance for 5 years for final approval. EIS has been used previously in the LO-MSD laboratories on bare metals and on ZRP's. The samples formerly used for testing were flat, 0.16 cm (1/16 in) thick carbon steel coupons, 1.59 cm (5/8 in) in diameter. These previous EIS measurements were collected after various immersion times in 3.55% NaCl and did not include atmospheric exposure. This investigation explores the use of EIS in combination with atmospheric exposure at the beach corrosion test site as a short-term method for analyzing the performance of ZRP's.

2.3 Paints containing zinc dust have been used since the middle of the last century.' The zinc dust was originally combined with zinc oxide as a graying pigment. The basic nature of zinc and its oxides caused reactions with acid sites present in the natural polymers used as binding materials at that time. These reactions resulted in premature polymerization. The advent of synthetic, non-acid functional binders made possible the high pigment loading of zinc.[2] This development gave rise to a class of coatings referred to as zinc-rich paints. These coatings contain a high percentage by weight of zinc particles (between 75% and 95%). The binder may be either organic (e.g., epoxy, chlorinated rubber), or inorganic (e.g., a solvent-based ethyl silicate or a water-based inorganic silicate). Initially, the zinc provides cathodic protection to the steel substrate (galvanic effect); whenever there is a break in the coating, the cathodic action tends to protect the steel substrate from corrosion. Many times, where scratches or damage to an inorganic zinc coating have occurred, the zinc reaction products have proceeded to fill in the damaged area and seal it against further exposure." As exposure time increases, however, the galvanic action becomes less effective. The deposition of inhibiting zinc compounds at the base of the coating pores, followed by the sealing of the porous structure by the zinc corrosion products, results in what is referred to as the barrier mechanism of protection. The galvanic and the barrier effect both must undoubtedly occur to ensure long-term protection of the steel substrate.[4,5]

3.0 MATERIALS AND METHODS

3.1 A model 378 electrochemical impedance system manufactured by EG&G Princeton Applied Research Corporation was used for all electrochemical measurements. Electrochemical measurements were performed on 10.16 cm x 15.24 cm x 0.32 cm (4 in x 6 in x 1/8 in) carbon steel test panels. Twenty-one panels were coated with the ZRP's listed in Table 1. The materials included in this investigation had been rated previously at the 36-month exposure point to determine their degree of corrosion performance on a scale of 1 to 10 according to ASTM D610, with 10 being the highest rating; this rating is included in Table 1.

TABLE! 1 - MATERIALS TESTED, CODE, TYPE, AND RUST GRADE EVALUATION

COATING	CODE	TYPE	RATING
Ameron D-21-9	A	SB	10.00
Devoe Catha-Coat 302H	B	SB	1.25
Sherwin Williams Zinc Clad II	C	SB	10.00
Ameron D-4	D	WB	9.50
Ameron D-21-5	E	WB	5.75
Briner V-65	F	WB	10.00
Carboline CZ-D7	G	WB	10.00
DuPont Ganicin 347 WB	H	WB	10.00
Inorganic Coatings IC-531	I	WB	9.75
Porter TQ-4374H	J	WB	8.63
Southern Coatings Chemtec 600	K	WB	9.88
Subox Galvanox IV	L	SB	9.38
Byco SP-101	M	SB	8.13
Carboline CZ-11	N	SB	10.00
Coronado 935-152	O	SB	6.38
Devoe Catha-Coat 304	P	SB	10.00
Glidden Glid-Zinc 5530	Q	SB	8.63
Glidden Glid-Zinc 5536	R	SB	3.25
Koppers 701	S	SB	8.00
Subox Galvanox V	T	SB	4.50
Tnemec 90E-75	U	SB	8.75
WB = Water-based (inorganic silicate)			
SB = Solvent-based (ethyl silicate)			

3.2 The panels were mounted on an EG&G Princeton Applied Research Model K0235 Flat Cell (see Figure 1) with a working electrode area of 1 cm^2 (0.15 in'). The flat cell consists of a flat cylinder clamped horizontally between two end plates. One end plate houses the working electrode and the other houses the platinum counter electrode. The silver/silver chloride reference electrode is housed in a Luggin well with a Luggin capillary protruding from the bottom of the well.

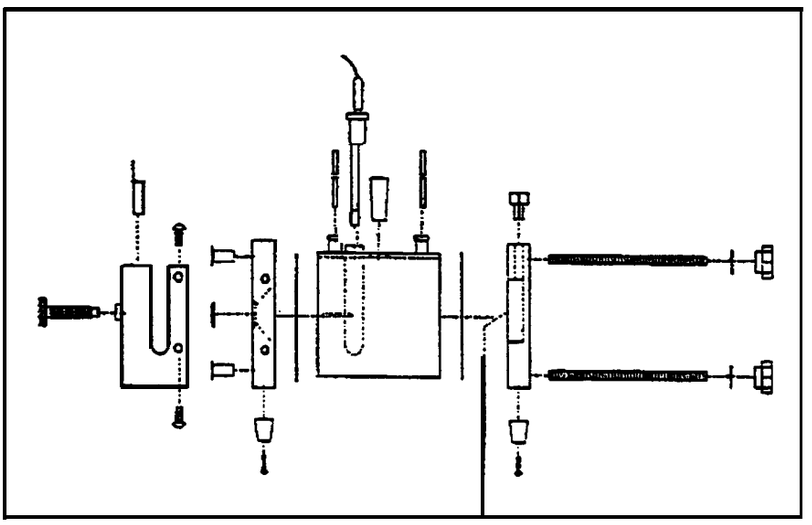

Figure 1 - Exploded View of Flat Cell

3.3 EIS data were collected after 1 hour immersion time in 3.55% NaCl. Data were gathered in the frequency range from 100 kHz to 0.01 Hz using the auto execute option of the M388 electrochemical analysis software. Three experiments were performed in a sequence covering the specified frequency range, and the data were automatically merged and saved. The frequency ranges for the three experiments were 100 kHz to 5 Hz, 10 Hz to 0.1 Hz, and 0.1 Hz to 0.01 Hz. The AC amplitude used for the experiments was 10 mV. After an initial set of measurements before atmospheric exposure, the panels were mounted on a rack (Figure 2) and taken to the Beach Corrosion Test Site (Figure 3) for a specified length of time. At the end of this time, the panels were brought back to the laboratory for a new set of measurements. This cycle was repeated every week for a total of 4 weeks of exposure initially. Subsequent measurements were performed after 8 weeks and 1 year of atmospheric exposure.

3.4 Corrosion potential as well as Bode magnitude (showing the logarithm of the modulus of the impedance, $\log |Z|$, as a function of the logarithm of frequency), Bode magnitude/phase angle (showing the phase angle as a function of the logarithm of frequency), and Nyquist plots (showing the negative of the imaginary impedance as a function of real impedance) of the data were obtained for each

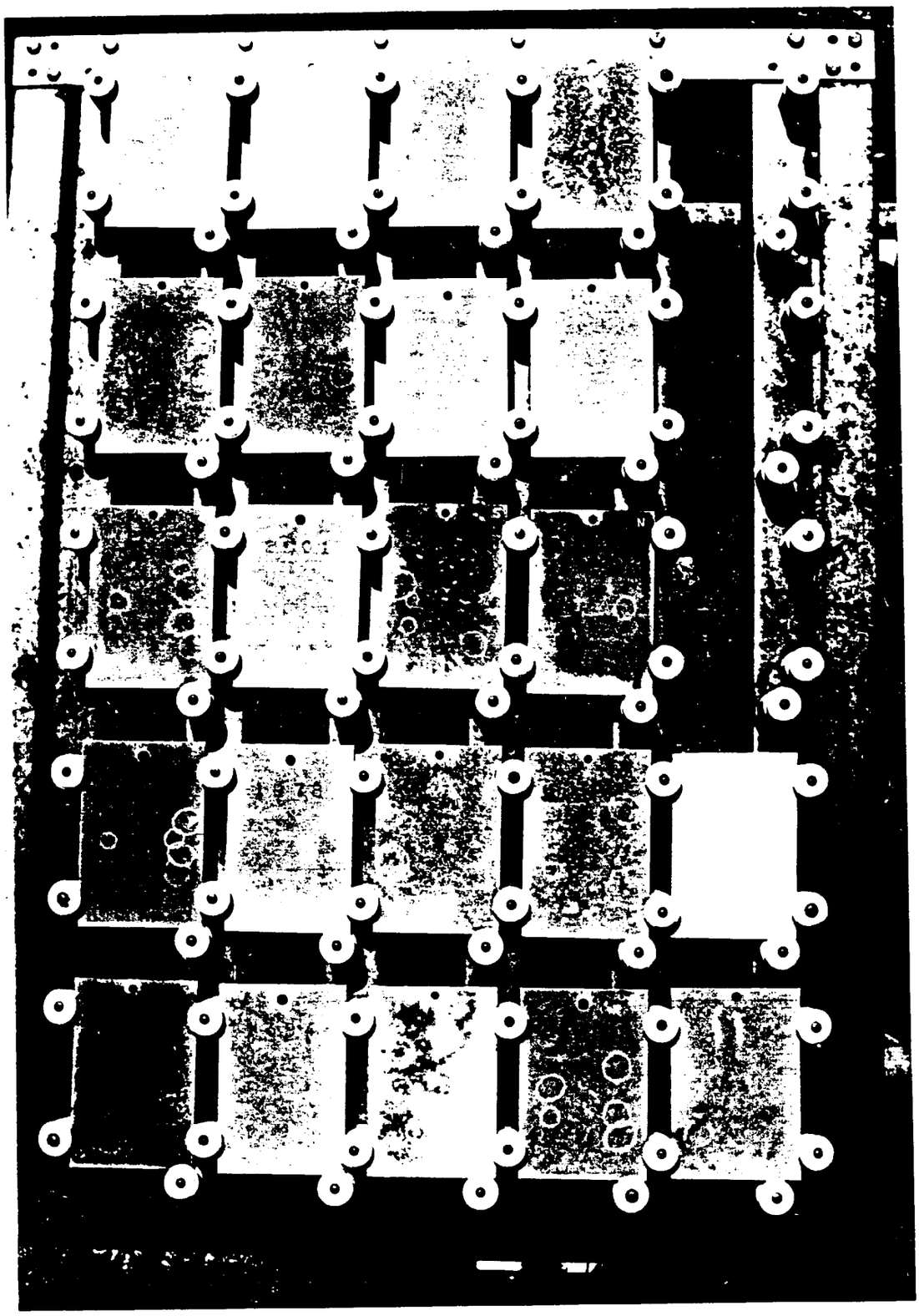

Figure 2 - Test Panels Mounted in Exposure Rack

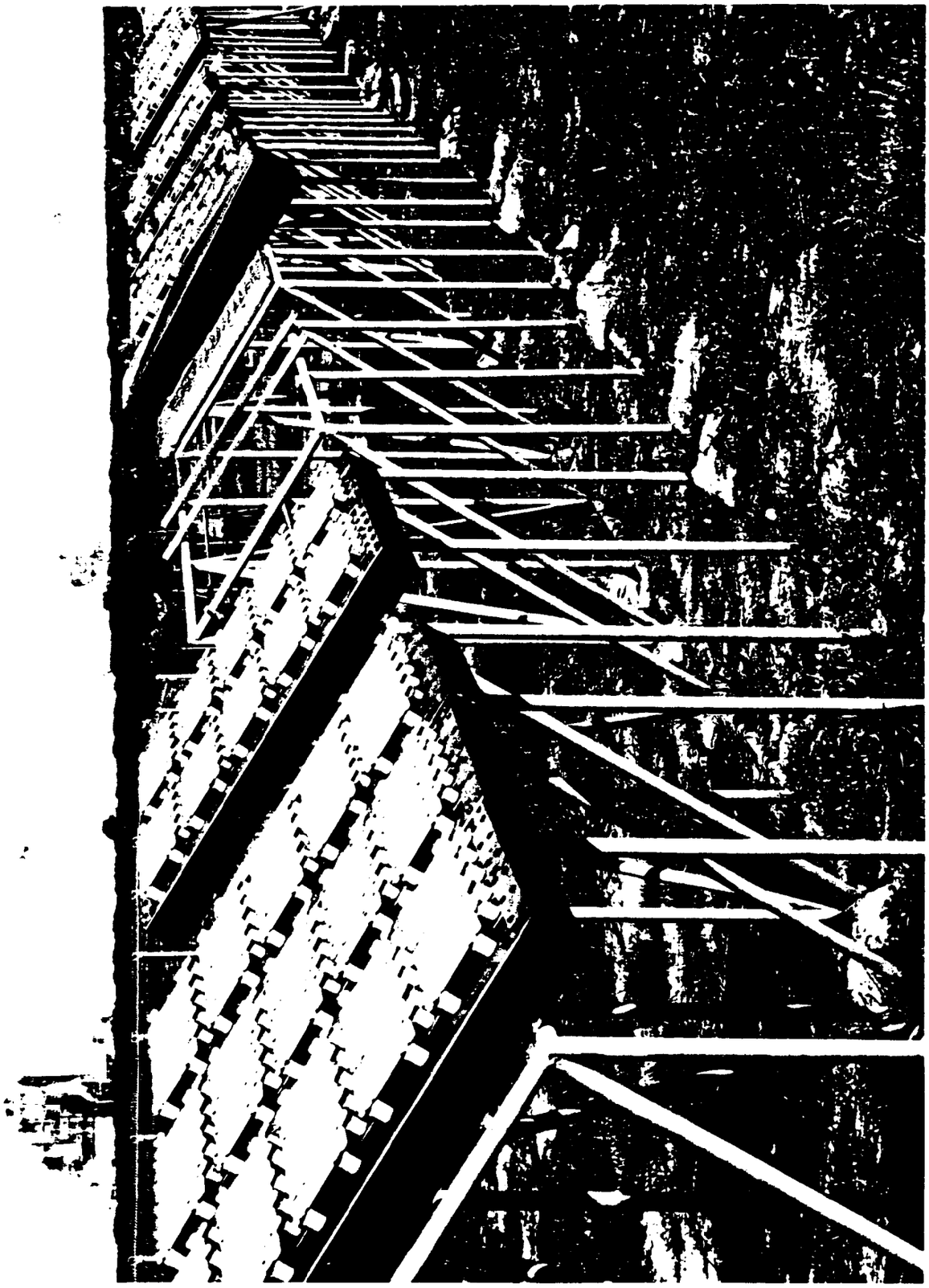

Figure 3 - Exposure Racks at KSC Beach Corrosion Test Site

coating after various times of atmospheric exposure. The impedance data were analyzed using the Equivalent Circuit computer simulation program by B. A Boukamp[6] with the purpose of identifying parameters that could be used to predict the long-term performance of ZRP's.

4.0 RESULTS AND DISCUSSION

4.1 The variation of the corrosion potential with time of atmospheric exposure for the 21 coatings included in this investigation is presented in Table 2. Graphical representations of the variation of the corrosion potential with time of atmospheric exposure are presented in Figure 4 for four representative coatings (A, P, R, and T).

4.2 The change in the corrosion potential with time is a useful indicator of the galvanic mechanism of protection for the coating. The corrosion potential of steel in 3.55% NaCl quoted in various standards and codes of practice' is -0.735 V Ag/AgCl (-0.780 V versus SCE). At or below this potential, the corrosion of the steel is reduced to approximately zero. Coatings A and P exhibited galvanic protection for a time greater than 8 weeks but less than 1 year. Coatings R and T exhibited corrosion potentials above the protection potential for steel after 2 weeks of atmospheric exposure, thus indicating their failure at protecting the steel galvanically; however, measurements of corrosion potential variation with time provide no estimate of the performance of the coating after the cessation of the cathodic protection mechanism. Coatings K and 0 exhibit an unexpected variation of the corrosion potential with time of atmospheric exposure. Coating K exhibits a corrosion potential above -0.735 V Ag/AgCl before the 1 year measurement. A possible interpretation of the high rating of this coating is that its galvanic mechanism of protection takes longer to develop. Coating 0 shows the variation in the corrosion potential with time of atmospheric exposure expected for a high rated coating even though it has a low rating. Testing of this coating at the Beach Corrosion Test Site resulted in a high rating during the first year before it dropped to a lower rating. It can be hypothesized that a strong galvanic effect does not necessarily result in the formation of a good barrier.

4.3 Another indication of the galvanic mechanism of protection is obtained by analyzing the EIS data. Figure 5 is typical of the Bode plots obtained for ZRP's. Upon initial immersion in 3.55% NaCl (prior to atmospheric exposure), the coating is protecting the steel galvanically. The low frequency intercept in the Bode plot is related to the corrosion of the zinc dust in the coating. The magnitude of the impedance modulus is related to the rate of corrosion of the zinc dust: the smaller the impedance, the greater the rate of corrosion of the zinc and the greater its protective galvanic effect. Upon atmospheric exposure, the Bode plot changes to include what has been described as the barrier mechanism of

TABLE 2 - VARIATION OF CORROSION POTENTIAL (VOLTS) WITH TIME OF ATMOSPHERIC EXPOSURE

COATING	INITIAL	ONE WEEK	TWO WEEKS	THREE WEEKS	FOUR WEEKS	EIGHT WEEKS	ONE YEAR
Ameron D-21-9	-1.029	-1.025	-0.980	-0.947	-0.947	-0.898	-0.409
Devoe Catha-Coat 302H	-0.004	-0.894	-0.143	-0.328	0.002	-0.084	-0.536
Sherwin Williams Zinc Clad II	-1.015	-1.024	No Data	-0.923	-0.907	-0.836	-0.520
Ameron D-4	-0.990	-0.899	-0.767	-0.816	-0.625	-0.800	-0.727
Ameron D-21-5	-0.249	-0.552	-0.575	-0.155	-0.248	-0.457	-0.769
Briner V-65	-1.009	-1.030	-0.995	-0.976	-0.904	-0.877	-0.561
Carboline CZ-D7	-0.777	-0.117	-0.829	-0.869	-0.789	-0.879	-0.394
DuPont Ganicin 347 WB	-0.895	-0.758	-0.968	-0.903	-0.692	-0.853	-0.688
Inorganic Coatings IC-531	-0.846	-0.725	-0.881	-0.867	-0.692	-0.810	-0.720
Porter TQ-4374H	-0.992	-0.982	-0.944	-0.935	-0.766	-0.852	-0.414
S. C. Chemtec 600	-0.524	-0.571	-0.560	-0.616	-0.305	-0.499	-0.742
Subox Galvanox IV	-0.988	-0.999	-0.979	-0.935	-0.968	-0.889	-0.603
Byco SP-101	-1.013	-1.025	-0.964	-0.965	-0.718	-0.788	-0.270
Carboline CZ-11	-0.814	-1.021	-1.008	-0.949	-0.796	-0.925	-0.913
Coronado 935-152	-1.035	-1.022	-0.956	-0.926	-0.959	-0.862	-0.407
Devoe Catha-Coat 304	-0.987	-0.995	-0.939	-0.930	-0.766	-0.894	-0.449
Glidden Glid-Zinc 5530	-1.016	-1.011	-0.957	-0.929	-0.953	-0.888	-0.393
Glidden Glid-Zinc 5536	-0.768	-1.015	-0.490	-0.771	-0.269	-0.909	-0.460
Koppers 701	-0.975	-0.999	-0.937	-0.950	-0.821	-0.901	-0.524
Subox Galvanox V	-1.002	-1.020	-0.244	-0.584	-0.468	-0.843	-0.651
Tnemec 90E-75	-0.983	-0.686	-0.861	-0.773	-0.520	-0.513	-0.336

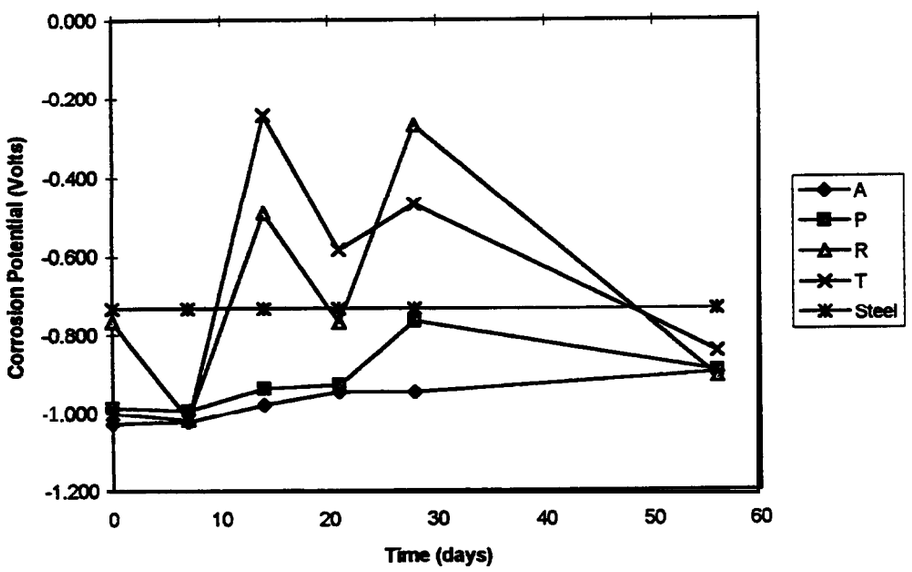

Figure 4 - Variation of Corrosion Potential with Time

protection Figure 5 shows the increase in impedance that corresponds to the decrease in the galvanic effect and the increase of the barrier mechanism of protection. The shape of the Bode plot also shows how the capacitive and resistive characteristics of the coating change with duration of atmospheric exposure. The capacitive behavior decreases as the time of atmospheric exposure increases.

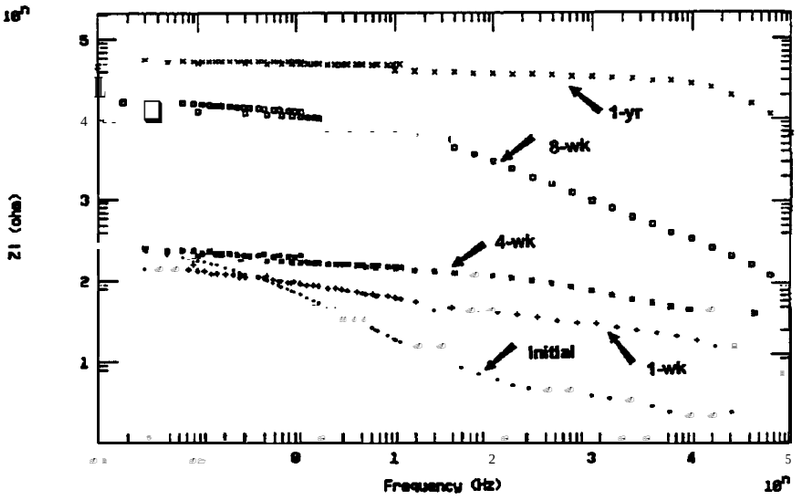

Figure 5 - Bode Plots for Coating A

4.4 To extract information on the galvanic as well as on the barrier mechanism of protection from the data generated in this investigation, the impedance spectra were analyzed using a computer simulation program.[6] The equivalent circuit program allows the design of a theoretical model of the impedance experiment by mathematically simulating an electronic network. The program generates a theoretical inpedance plot for the equivalent circuit designed, overlays this plot on the experimental results, performs a statistical analysis of the fit of the model to the data, and automatically adjusts the component values in the model to optimize its fit to the data The equivalent circuit $R_1(R_2C(R_3W))$[8] shown in Figure 6 provided a satisfactory fit for the data (see simulation curves in Figures 7, 8 and in the Appendix). The letters R, C, and W denote a resistor, capacitor, and Warburg impedance, respectively.

4.5 Table 3 lists the values obtained for R_2 for all the materials tested. Graphical representation of the variation of R_2 with time of atmospheric exposure is presented in Figure 9 for four representative coatings (A, P, R, and T). During the early stages of atmospheric exposure, R_2 represents the galvanic mechanism of protection involving the corrosion of the zinc. After this period, the resistance is equivalent to the magnitude of the film resistance. Its increase is due to the build-up of zinc corrosion products responsible for the barrier effect. This trend holds

for coating P up to 56 days of atmospheric exposure, and for coatings A and T up to 28 days of atmospheric exposure. The change in the value of R_2 for coating T was not as gradual as it was for coatings A and P, perhaps resulting in the formation of a barrier that was not as effective in protecting the steel.

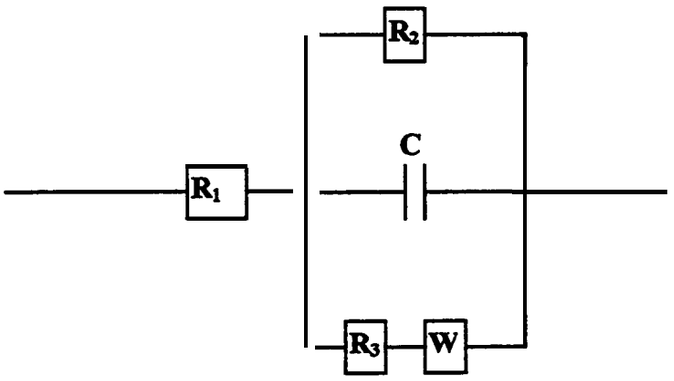

Figure 6 - Equivalent Circuit Model for ZRP's.

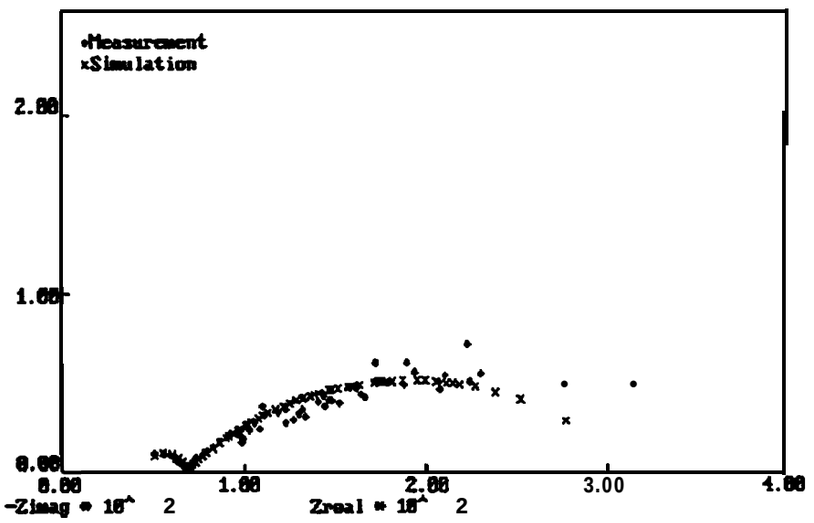

Figure 7 - Nyquist Plot of Equivalent Circuit Fit for Coating Q

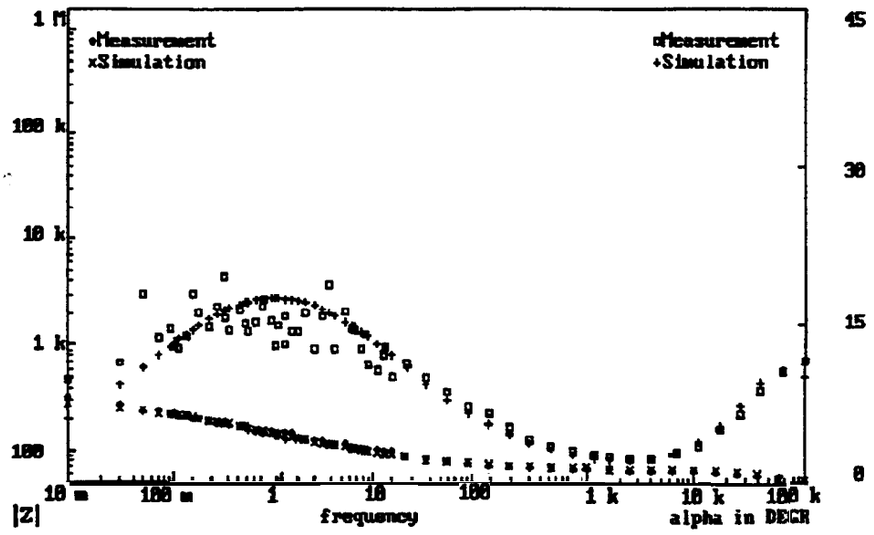

Figure 8 - Bode Plot of Equivalent Circuit Fit for Coating Q

TABLE 3 - VARIATION OF R_2 (OHMS) WITH WITH TIME OF ATMOSPHERIC EXPOSURE

COATING	INITIAL	ONE WEEK	TWO WEEKS	THREE WEEKS	FOUR WEEKS	EIGHT WEEKS	ONE YEAR
Ameron D-21-9	3.72E+02	1.50E+02	1.14E+04	1.14E+04	2.50E+05	1.52E+04	5.19E+04
Devoe Catha-Coat 302H	7.08E+06	1.25E+05	6.97E+06	1.11E+06	9.61E+06	6.42E+06	6.56E+07
s. W. Zinc Clad II	1.86E+02	3.76E+02	1.81E+04	3.28E+02	9.12E+03	3.48EU-M	3.38E+03
Ameron D-4	4.72E+01	5.56E+02	2.80E+04	5.90E+03	3.25E+05	1.18E+04	1.27E+05
Ameron D-21-5	9.34E+02	1.73E+05	No Data	2.16E+06	5.26E+04	1.83E+03	1.97E+04
Briner V-65	1.57E+02	3.72E+02	3.28E+02	6.60E+02	1.20E+03	7.58E+03	6.96E+03
Carboline CZ-D7	7.93E+03	1.10E+07	1.75E+03	1.75E+03	2.31E+05	1.80E+03	5.31E+07
DuPont Ganicin 347	5.36E+02	2.90E+03	2.43E+02	4.00E+02	7.23E+02	2.53E+03	1.49E+04
IC-531	1.07E+03	1.43E+02	3.54E+02	9.32E+02	1.69E+03	1.54E+03	7.22E+03
Porter TQ-4374H	6.66E+02	7.61E+02	No Data	4.29E+03	6.58E+03	4.79E+03	4.58E+03
S. C. Chemtec 600	3.75E+04	3.43E+05	1.29E+04	1.19E+06	2.10E+05	2.86E+03	1.59E+06
Subox Galvanox IV	4.57E+02	1.25E+03	5.93E+02	1.32E+03	2.48E+03	3.44E+03	1.97E+03
Byco SP-101	5.95E+02	3.40E+02	2.32E+02	7.13E+02	5.81E+05	4.45E+03	1.19E+05
Carboline CZ-11	1.00E+00	3.97E+02	3.10E+02	4.66E+04	3.20E+03	1.28E+03	3.84E+04
Coronado 935-152	5.71E+01	7.08E+02	3.16E+02	9.15E+02	1.57E+03	1.50E+04	3.31E+03
Devoe Catha-Coat 304	1.89E+02	4.97E+02	9.88E+02	2.33E+03	3.70E+03	2.58E+04	2.22E+04
Glidden Glid-Zinc 5530	1.97E+02	2.71E+02	1.55E+04	3.01E+02	3.53E+02	3.62E+04	7.56E+05
Glidden Glid-Zinc 5536	1.65E+06	9.28E+02	1.07E+05	4.49E+04	2.98E+06	8.6;7E+04	5.57E+06
Koppers 701	1.68E+02	5.31E+03	1.02E+05	1.44E+03	1.29E+03	3.25)E+04	5.32E+03
Subox Galvanox V	3.77E+02	5.29E+02	1.68E+06	1.49E+06	1.21E+06	3.51E+03	2.21E+04
Tnemec 90E-75	5.05E+04	No Data	1.44E+03	2.62E+03	2.60E+03	4.84E+03	4.50E+03

4.6 Table 4 lists the values obtained for capacitance (C) for all the materials tested. The capacitance variation with time of atmospheric exposure is shown graphically in Figure 10 for representative coatings A, P, R, and T. Coatings A and P exhibit initial capacitances on the order of 10^{-4} farad. Both coatings show a gradual change toward lower values of capacitance in the order of 10^{-10} farads. Lower capacitance values can be attributed to a decrease in the water content of the protective film. The water is excluded by the accumulation of the zinc corrosion products in the pores of the film. Coatings R and T exhibit initial capacitances that are lower than those for coatings A and P. The change in capacitance with time of atmospheric exposure for coatings R and T is not as pronounced as was observed for coatings A and P. This behavior may be attributed to the fact that coatings R and T do not form a barrier that affords as effective long-term protection of steel as the barrier formed by coatings A and P.

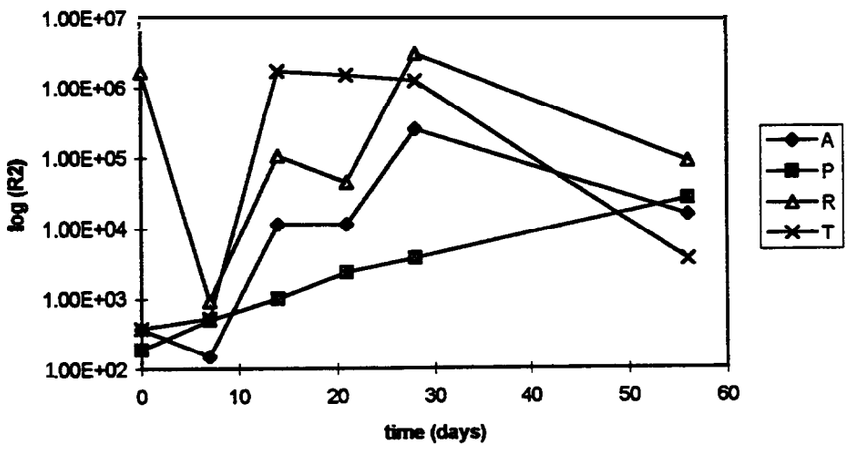

Figure 9 - Variation of R_2 with Time

4.7 Table 5 lists the variation of the phase angle at 1 Hz with time of atmospheric exposure for all materials tested. The variation of the phase angle at 1 Hz with time of atmospheric exposure is shown graphically in Figure 11 for representative coatings A, P, R, and T. This measurement is used to determine if the material displays capacitive or resistive behavior. If the initial phase angle is comparatively high at 1 Hz, this indicates capacitive behavior. This behavior would be consistent with a primer film that is very porous and contains water. The water within the porous film charges like a capacitor, and this response is detected by EIS. The greater the value of the phase angle at a given frequency, the more porous the film and greater the water content. Coatings A and P show this behavior. Coatings R and T exhibit initial phase angles at 1 Hz that are lower, thus indicating lower porosity and lower capacitance. The decrease of the phase angle at 1 Hz with time of atmospheric exposure shows that coatings A and P exclude water and

become less porous with aging. Coatings R and T exhibit a behavior characterized by a phase angle that starts low and fluctuates up and down upon atmospheric exposure.

4.8 Comparison of phase angle data before and after atmospheric exposure reveals the transition characteristics of the inorganic zinc primer film. A transition to a lower phase angle upon weathering (e.g., <10 deg) at 1 Hz indicates the film is becoming more of a barrier. This low value of phase angle indicates a more resistive behavior, which is related to the reduction in film porosity and exclusion of water. This would be consistent with the formation of barrier qualities of the primer coating.

TABLE 4 - VARIATION OF C (FARADS) WITH TIME OF ATMOSPHERIC EXPOSURE

COATING	INITIAL	ONE WEEK	TWO WEEKS	THREE WEEKS	FOUR WEEKS	EIGHT WEEKS	ONE YEAR
Ameron D-21-9	3.06E-04	1.51E-06	8.66E-10	8.66E-10	2.29E-10	1.37E-	2.14E-10
Devoe302H	2.11E-10	5.45E-10	1.44E-10	3.34E-10	1.29E-10	1.89E-10	1.34E-10
S. W. Zinc Clad II	7.91E-06	3.78E-06	3.29E-08	1.68E-08	2.89E-09	2.10E-09	2.28E-09
AmexonD-4	4.25E-05	1.55E-08	2.91E-09	7.07E-10	2.44E-10	1.40E-09	2.80E-10
Ameron D-21-5	3.16E-07	4.01E-10	No Data	5.46E-10	1.09E-09	7.38E-08	6.87E-09
Briner V-65	1.47E-04	6.23E-05	7.38E-06	1.45E-06	1.42E-07	1.11E-08	9.99E-09
Carboline CZ-D7	5.43E-07	3.14E-10	2.03E-07	2.03E-07	5.60E-10	6.88E-08	2.31E-10
347 WB	1.05E-07	5.01E-07	1.99E-07	2.33E-07	1.83E-07	1.49E-08	7.49E-09
IC-531	6.69E-08	7.00E-07	2.38E-06	1.96E-07	1.13E-07	3.40E-08	8.02E-09
Porter TQ-4374H	2.55E-06	1.67E-06	No Data	2.15E-06	1.06E-09	1.43E-08	9.17E-09
S. C. Chemtec 600	2.90E-08	5.88E-10	1.36E-08	6.69E-10	6.72E-10	3.21E-08	4.09E-10
Subox IV	2.99E-04	1.53E-04	2.51E-06	3.64E-06	1.44E-06	6.50E-07	2.04E-08
Byco SP-101	3.50E-09	9.26E-05	1.49E-07	9.72E-08	2.87E-10	1.62E-09	3.12E-10
Carboline CZ-11	1.84E-06	3.85E-07	7.44E-08	2.71E-10	5.57E-09	1.07E-07	2.63E-10
Coronado 935-152	1.38E-04	9.41E-05	6.25E-07	3.38E-09	6.81E-07	1.06E-08	2.48E-09
Devoe 304	5.52E-04	1.03E-05	4.30E-08	1.27E-08	5.23E-09	5.28E-09	2.04E-10
Glid-Zinc 5530	1.43E-04	1.35E-07	3.201E-10	6.89E-09	2.68E-08	4.99E-10	3.61E-10
Glid-Zinc 5536	2.78E-10	2.10E-08	2.41E-09	3.81E-09	3.01E-10	3.42E-10	3.59E-10
Koppers 701	9.44E-07	4.96E-09	MOE-10	6.09E-07	3.58E-07	1.93E-10	5.02E-09
Subox Galvanox V	2.76E-07	2.80E-07	1.31E-10	r 2.01E-10	2.18E-10	8.23E-08	2.45E-08
Tnemec 90E-75	1.58E- 1 0	No Data	3.44E-08	2.45E-08	1.21E-08	1.69E-08	3.31E-09

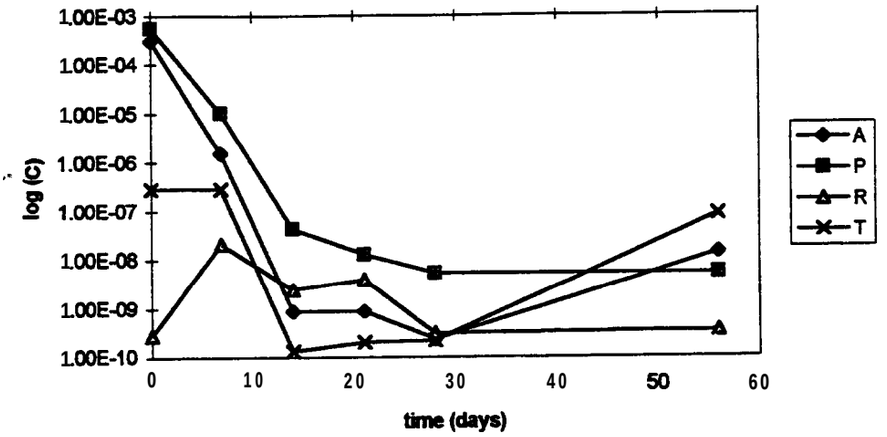

Figure 10 - Variation of Capacitance (C) with Time

TABLE 5 - VARIATION OF PHASE ANGLE (DEG) AT 1 HZ WITH TIME OF ATMOSPHERIC EXPOSURE

COATING	INITIAL	ONE WEEK	TWO WEEKS	THREE WEEKS	FOUR WEEKS	EIGHT WEEKS	ONE YEAR
Ameron D-21-9	44.5	15.6	3.7	6.1	2.7	10.4	0.6
Devoe Catha-Coat 302H	2.4	6.9	10.7	0.6	9.0	9.3	16.7
S. W. Zinc Clad II	26.1	31.5	38.8	3.5	3.5	3.5	3.7
Ameron D-4	13.9	11.2	8.0	1.0	1.8	9.2	0.7
Ameron D-21-5	59.8	8.6	8.6	31.1	27.4	14.8	12.1
Briner V-65	33.3	30.1	28.0	28.5	27.8	7.4	6.3
Carboline CZ-D7	32.4	52.6	31.6	28.5	3.8	27.1	35.1
347 WB	18.8	34.0	15.8	16.0	21.0	3.4	9.5
IC-531	21.2	39.1	37.5	15.3	19.1	7.2	6.9
Porter TQ-4374H	45.4	42.1	No Data	51.9	4.7	11.8	7.6
S. C. Chemtec 600	42.7	19.2	24.4	21.1	9.6	15.2	20.3
Subox Galvanox IV	43.6	43.9	34.1	29.5	33.4	32.4	5.6
Byco SP-101	5.0	9.7	12.2	15.2	13.7	13.7	4.6
Carboline CZ-11	36.5	25.0	12.7	1.9	3.7	23.6	0.8
Coronado 935-152	16.7	42.3	8.2	4.7	8.1	4.7	1.6
Devoe Catha-Coat 304	41.6	28.4	12.3	10.7	11.0	8.4	0.9
Glidden Glid-Zinc 5530	21.2	13.2	1.8	5.5	8.3	3.0	10.0
Glidden Glid-Zinc 5536	-8.1	21.6	25.0	17.5	16.4	0.2	29
Koppers 701	11.4	11.3	0.0	18.0	19.6	0.8	4.6
Subox Galvanox V	14.0	16.1	4.4	5.0	5.0	16.8	13.5
Tnemec 90E-75	0.0	0.0	4.8	4.5	3.3	6.0	3.3

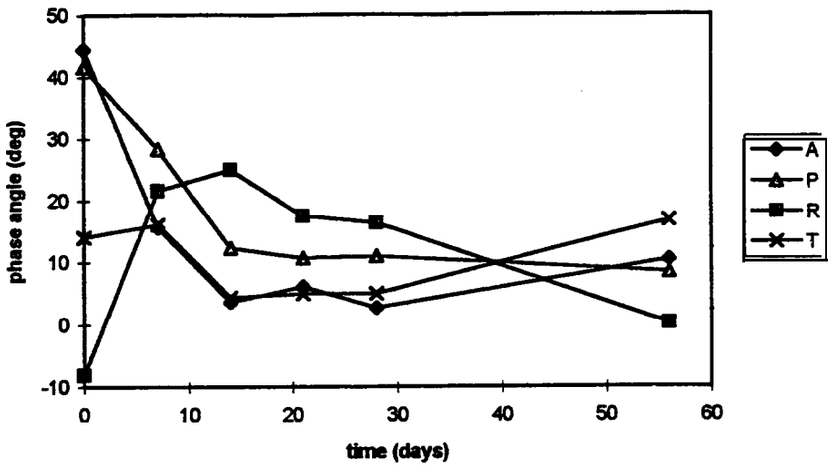

Figure 11 - Variation of Phase Angle (deg) with Time

4.9 Based on the variations of electrochemical parameters discussed, analysis of the data has revealed indications that certain behavior could predict long-term primer performance. Since a corrosion potential (Ecorr) of approximately -0.735 volts versus Ag/AgCl is the corrosion potential of bare steel in 3.55% NaCl, potentials more negative than this indicate cathodic influence of the zinc particles in the primer film. The more negative the potential (e.g., -1.000 volts versus Ag/AgCl), the greater the cathodic protection provided to the steel substrate. As seen from the Ewrr versus time data, generally the corrosion potential becomes more positive with outdoor exposure, indicating a transition to an alternate protection mechanism As shown in the data, this initial information gives no immediate indication of long-term performance, but does show that a material has the galvanic strength to protect the steel substrate in the short-term. Materials with initial potentials well above -0.735 volts have displayed some localized rusting and reduction in protection of scribed (damaged) areas in long-term corrosion tests at the Beach Corrosion Test Site. The variation of Ecorr with time of atmospheric exposure provides information on the galvanic mechanism of protection and is useful to distinguish between strongly galvanic materials and non-galvanic materials.

4.10 After evaluation of the corrosion potential as outlined above, the measurement of the initial R_2 is used to determine the magnitude of the initial zinc corrosion in the primer film. Primers that display an initial R_2 of less than 10^3 indicate relatively high rates of sacrificial zinc corrosion in the film for galvanic protection of the steel substrate. Materials with much higher R_2's (e.g., 10^5 ohms) could display a lack of initial galvanic protection to the substrate, based on the slower rate of zinc corrosion.

4.11 By comparing the initial to the aged R_2 for the same material, clues to the mechanisms of substrate protection are evidenced. If R_2 increases with time, this could indicate that the rate of corrosion of the zinc particles and the galvanic activity of the film is slowing. This would be consistent with the theory that these materials transition from galvanic to a more barrier-like protection with time.

4.12 Another measurement studied was the coating capacitance. When the initial capacitance is high (e.g., $>10^{-4}$ farads), water is present in the porous film. As was stated before, this water can charge in the pores of the film and act like a capacitor. The magnitude of this capacitance provides a qualitative measurement of the porosity of a particular primer film. Higher values would indicate more porosity, whereas lower values would indicate lower porosity.

4.13 When the initial capacitance is compared to the aged capacitance, the unique transformation of the primer film becomes clearer. If the aged capacitance becomes much lower (e.g., $<10^{-9}$ farads), the barrier qualities of the film are confirmed. As the capacitance values become lower, the overall quality of the barrier can be relatively quantified. The lower values indicate almost total exclusion of water, extremely low porosity, and potential long-term protection of the steel substrate by the particular primer film.

4.14 The variation of the phase angle at 1 Hz with atmospheric exposure seems to correlate with the transition from a galvanic mechanism to a barrier mechanism of protection, assuming that this transition is accompanied by a decrease in the porosity of the film. When this transition occurs, water is excluded from the watingandthedecrease in the phase angle signals the concurrent decrease in capacitive behavior that takes place.

5.0 CONCLUSIONS

5.1 The corrosion potential and the R_2 resistance are parameters indicative of the galvanic mechanism of protection. A corrosion potential below -0.735 V Ag/AgCl and an R_2 value that starts around 10^2 ohms and increases gradually with time of atmospheric exposure is indicative of good galvanic activity. It is hypothesized that this behavior results in the formation of a protective layer that has a better corrosion resistance.

5.2 The capacitance of the coating and the phase angle are related to the barrier mechanism of protection. Good coatings have capacitances and phase angles that decrease gradually as the protective film formed by zinc corrosion products becomes less porous. This decrease in porosity is accompanied by a decrease in the water content of the film, which results in lower capacitance and phase angle values. For example, among the four coatings selected as illustrative examples, the two coatings with high ASTM ratings had capacitance values that varied from

around 10^{-4} farads initially to around 10^{-10} farads at the l-year exposure point. Similarly, the phase angle at 1 Hz for these coatings showed a gradual decrease to around 10 deg. The coatings with the low ASTM ratings had initial capacitances that were significantly lower than 10^{-4} farads. The phase angle at 1 Hz was also lower initially for these coatings an exhibited a fluctuating change with atmospheric exposure.

5.3 During the analysis of this data, it was concluded that measuring a change in a single electrochemical property was not a useful way to predict long term performance; however, when several key measurements were used together interactively, a much better trend was found. Work will continue to attempt to explain and refine the change in measurement values as it relates to long term coating performance. The equivalent circuit $R_1(R_2C(R_3W))$ provided a satisfactory fit for the EIS data and will continue to be used for future analysis. It has been shown that there is a correlation between the long-term performance of zinc-rich primers and several parameters obtained from EIS measurements in combination with atmospheric exposure.

INVESTIGATORS::

L. M. CALLE, NASA/ASEE SUMMER FACULTY FELLOW

L. G. MACDOWELL, III, NASA, LO-MSD-1M

APPROVED:

S. H. MURRAY, LEAD ENGINEER, MATERIALS

[1]R. *Mallet,* Br. *Assoc. Advancement of Science* **10, 221(** 1840).

[2]J. E. 0. Mayne, and U. R Evans, *Soc. Chem., Ind. Rev. 22,* 109 (1944).

[3]C. G. Munger, ***Corrosion Prevention by Protective Coatings,*** National Association of Corrosion Engineers, 1984.

[4]S. Feliu, R Barajas, J. M. Bastidas and M. Morcillo, *J. Coatings Technol.* **61,** 63 (1989).

[5]S. Feliu, R Barajas, J. M. Bastidas and M. Morcillo, *J. Coatings Technol.* **61,** 71 (1989).

[6]B. Boukamp, Equivalent Circuit Programme, University of Twente, Netherlands.

[7]N.A.C.E, Rp-ol-69, w-05-75, w-06-75, w-01-76, U.S.A.

[8]S. E. Faidi, J. D. Scantlebury, P. Bullivant, N. T. Whittle, and R Savin, *Corrosion Science, 35,* 1319 (1993).

APPENDIX[1]

REPRESENTATIVE BODE, BODE MAGNITUDE/PHASE ANGLE, AND NYQUIST PLOTS

[1] Although seven plots were generated for each coating, only six were chosen for each figure based on clarity and goodness of fit from the equivalent circuit simulation.

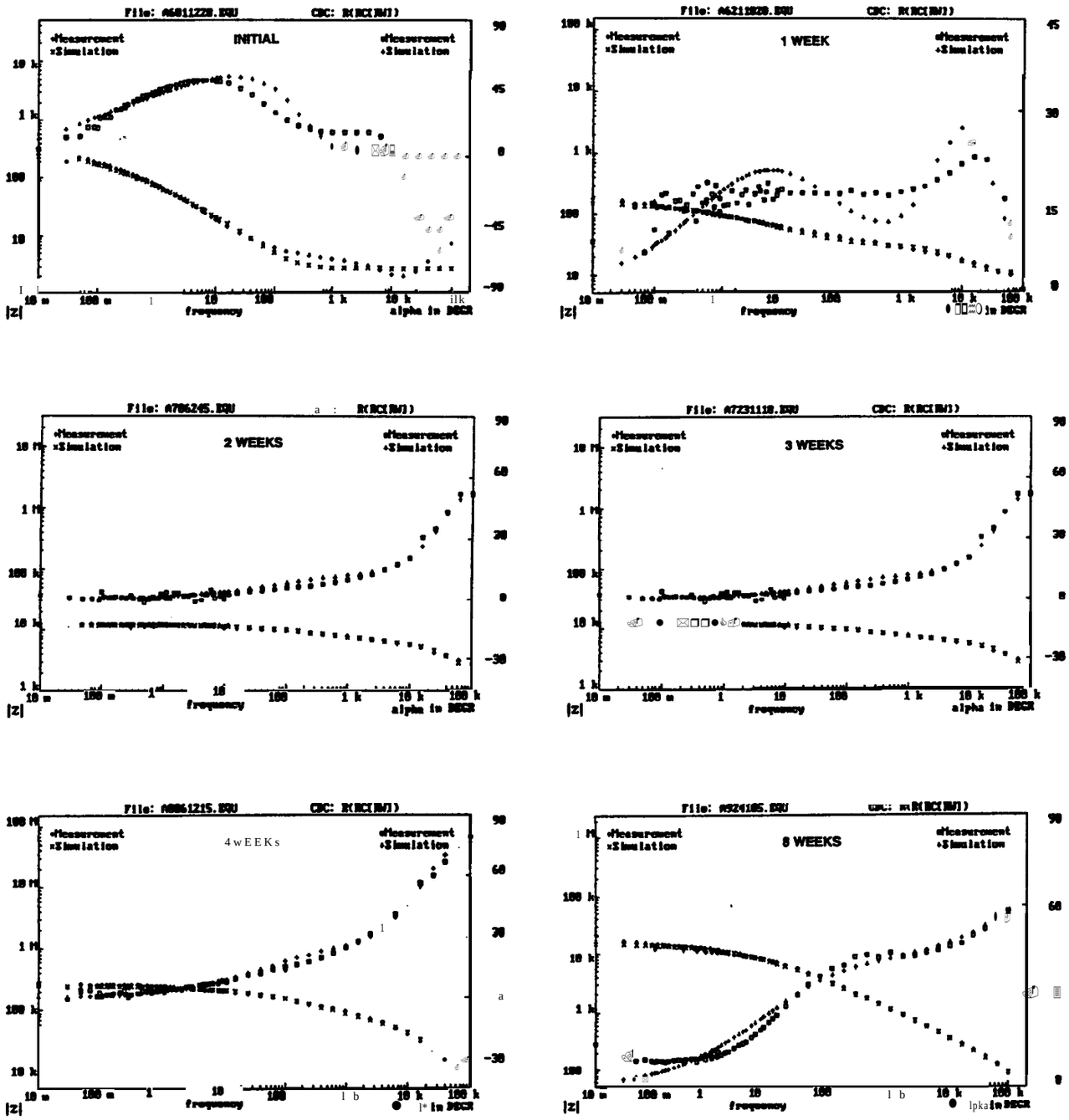

FIGURE A-l. BODE PLOTS OF AMERON D-21-9

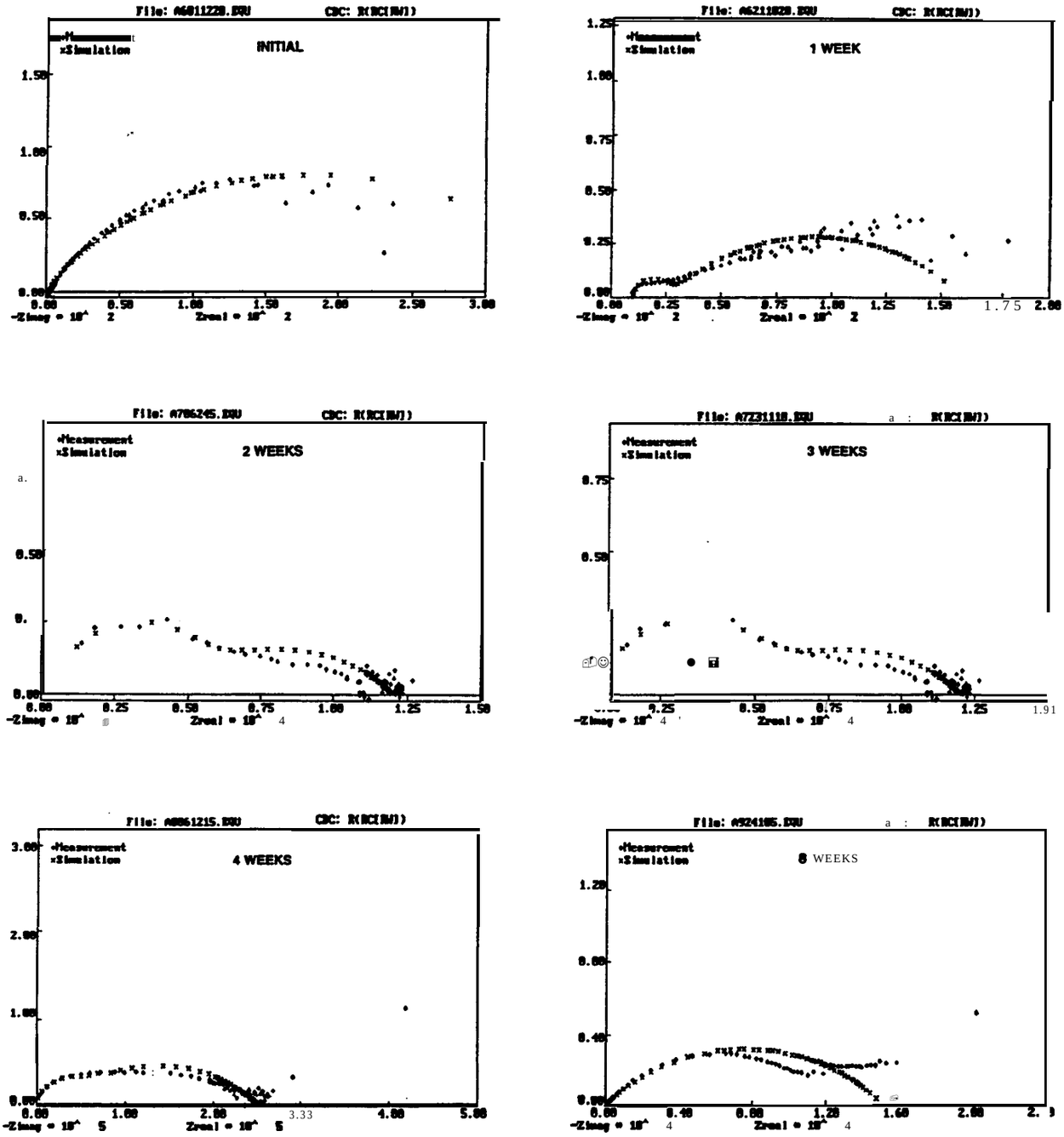

FIGURE A-2. NYQUIST PLOTS OF AMERON D-21-9

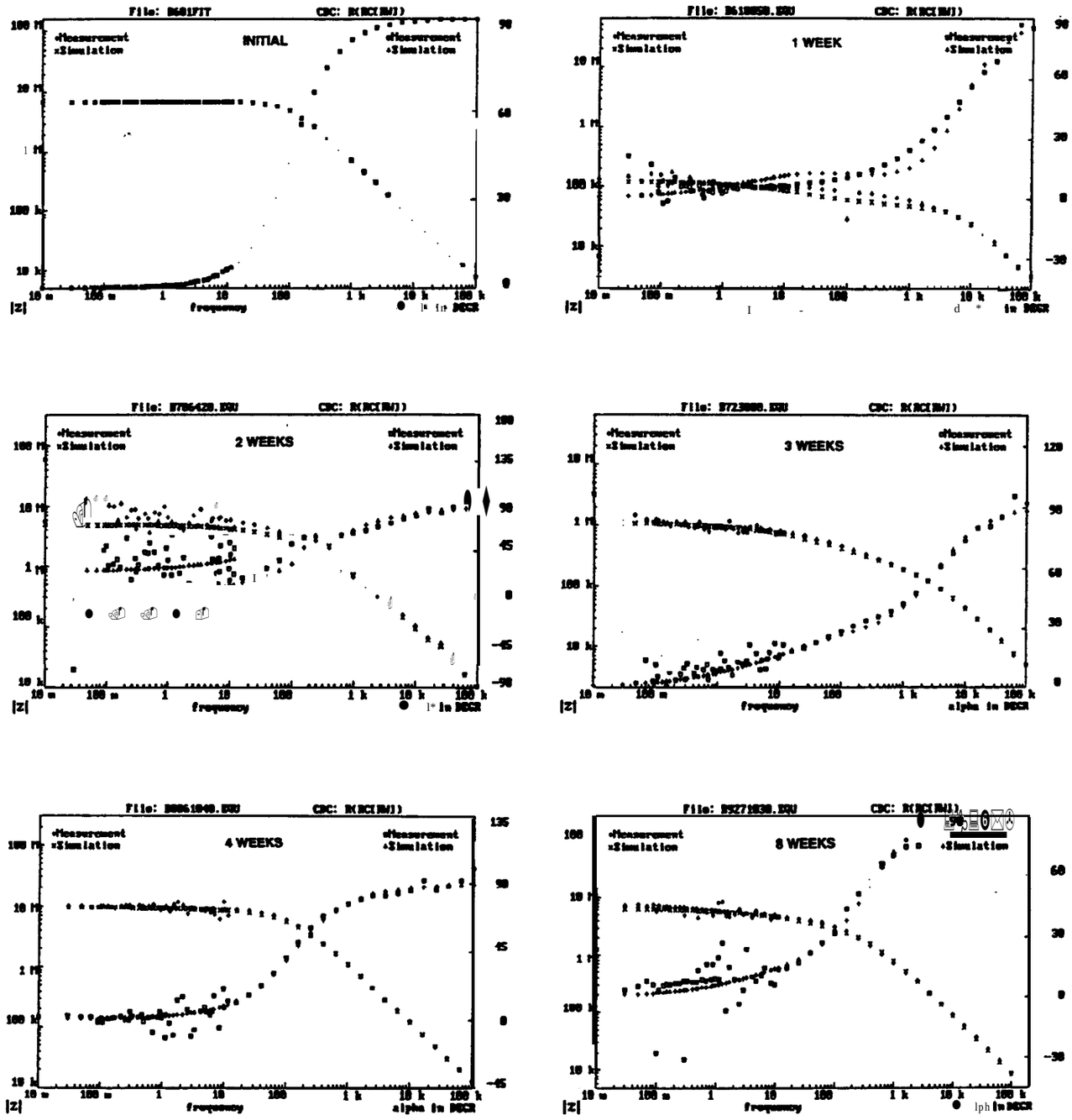

FIGUREA-3. BODEPLOTSOFDEVOECATHA-COAT302H

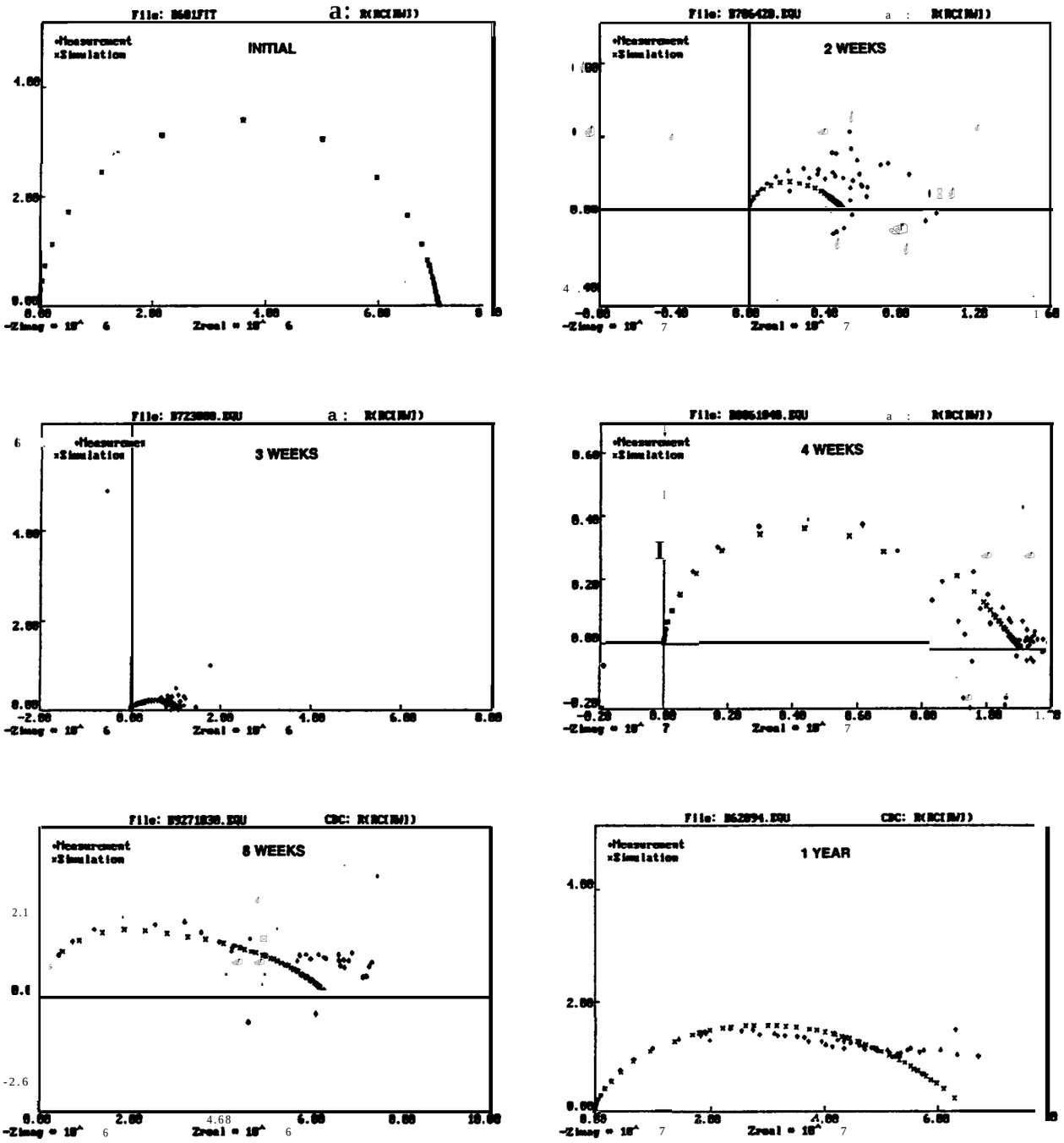

FIGURE A-4. NYQUIST PLOTS OF DEVOE CATHA-COAT 302H

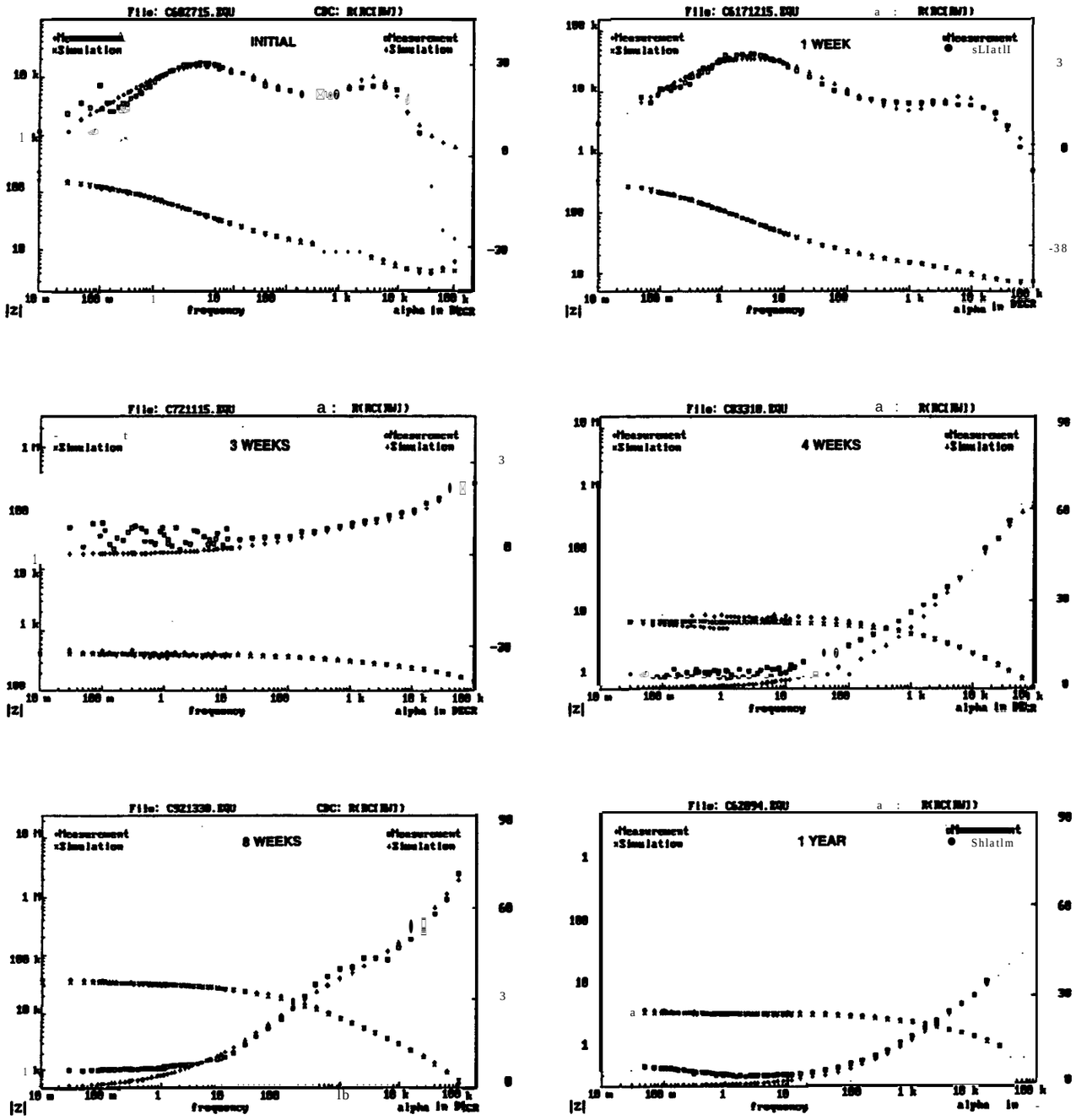

FIGURE A-5. BODE PLOTS OF SHERWIN WILLIAMS ZINC CLAD II

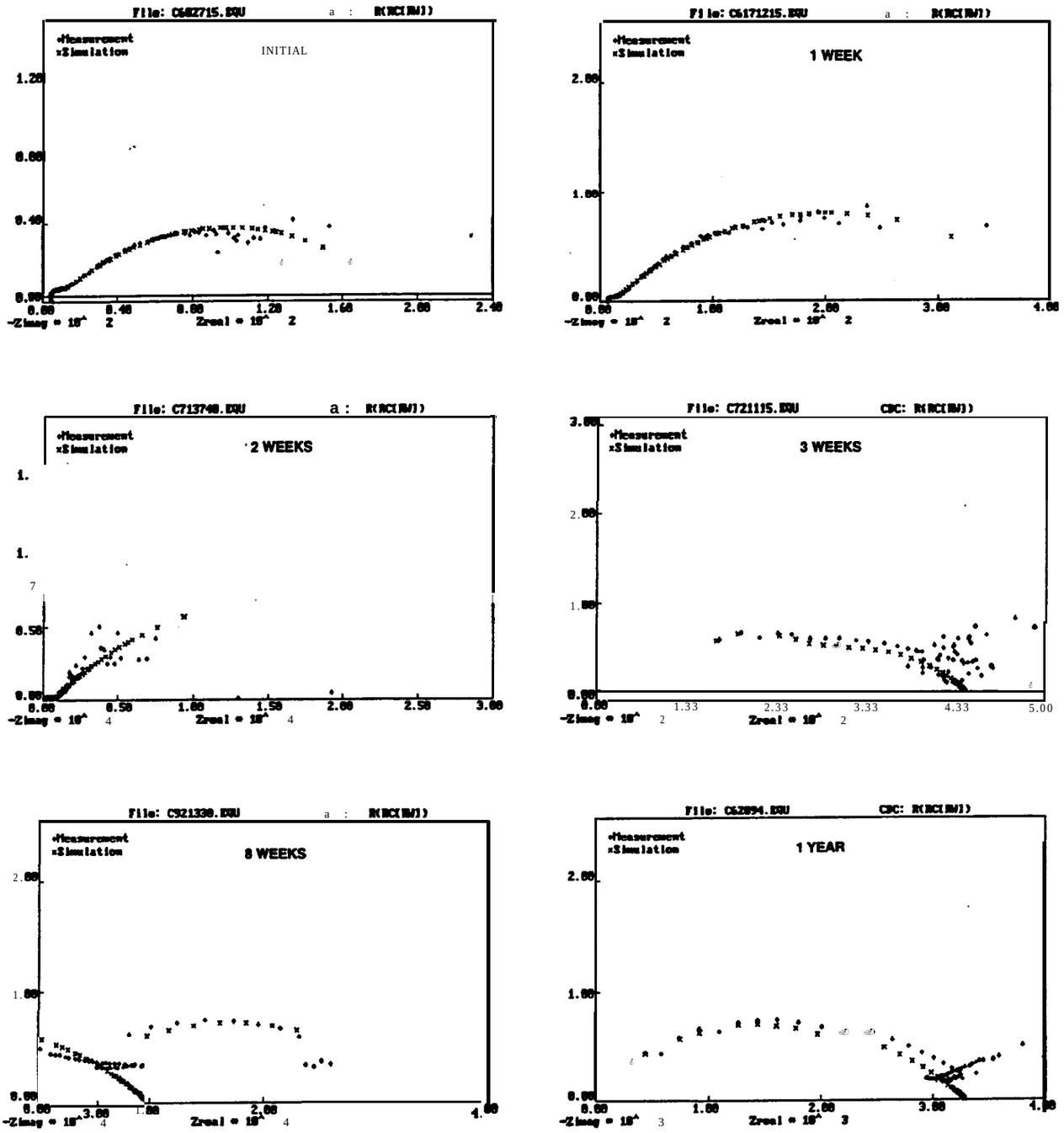

FIGURE A-6. NYQUIST PLOTS OF SHERWIN WILLIAMS ZINC CLAD II

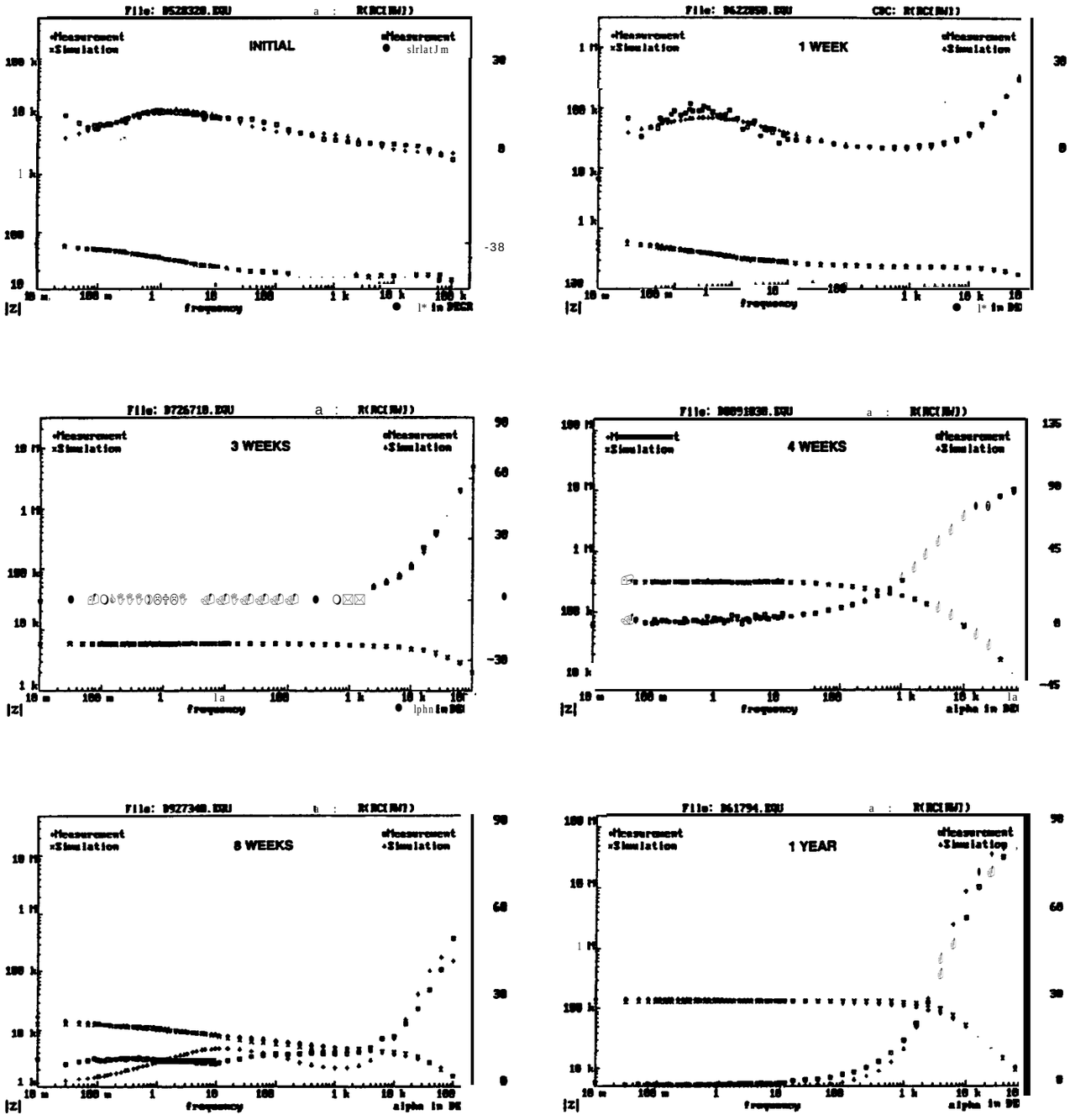

FIGURE A-7. BODE PLOTS OF AMERON D-4

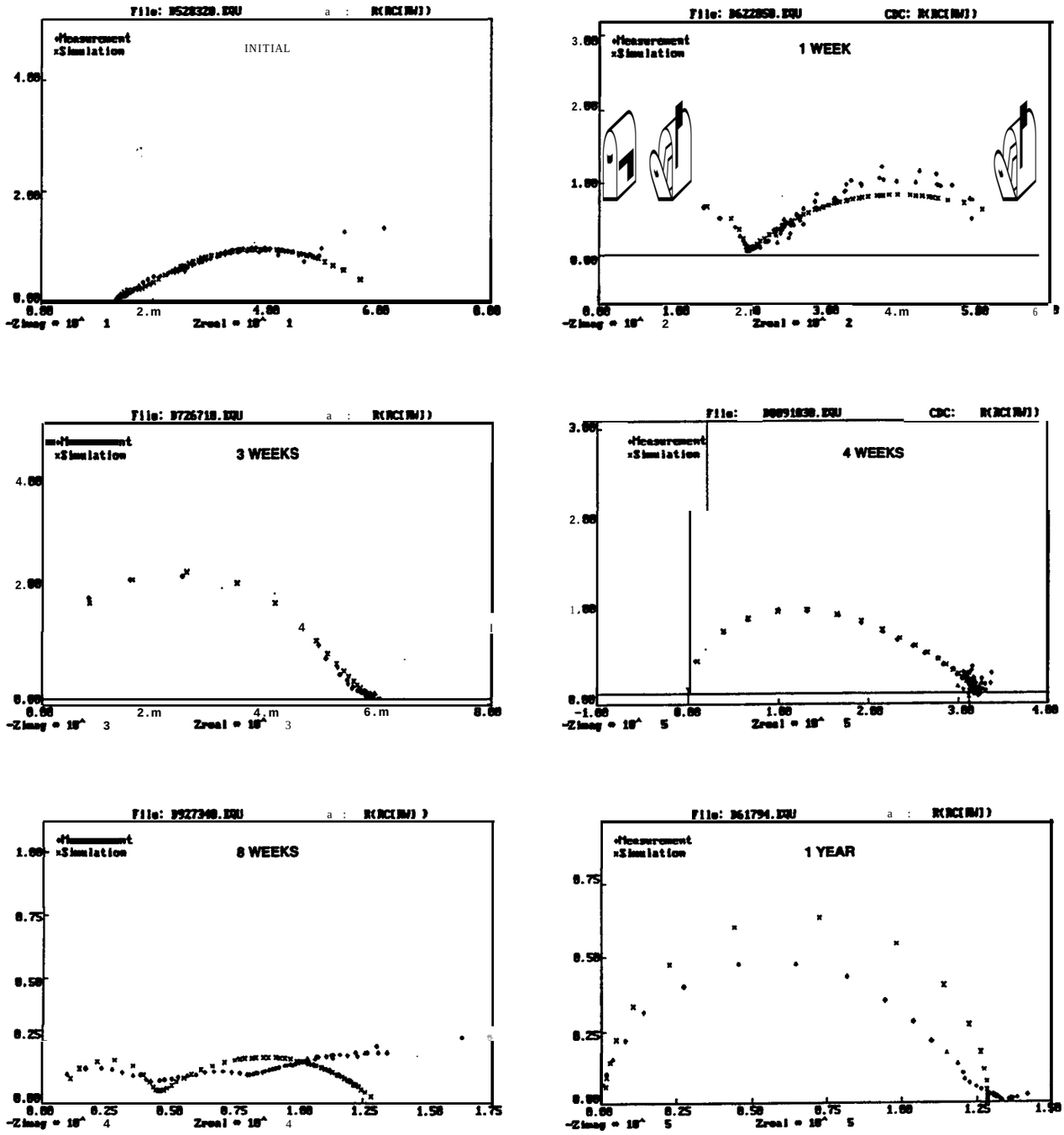

FIGURE A-8. NYQUIST PLOTS OF AMERON D-4

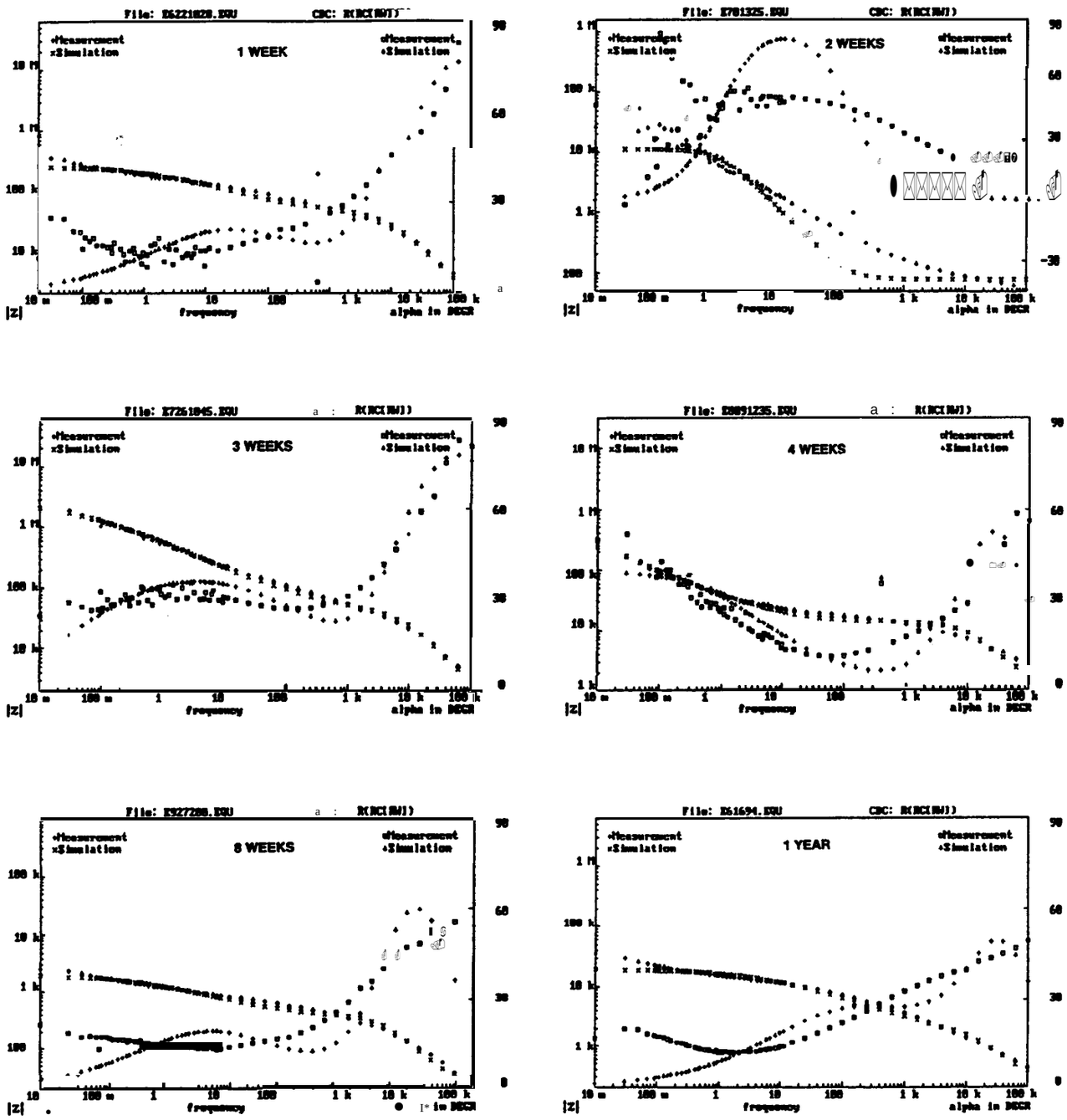

FIGURE A-9. BODE PLOTS OF AMERON D-21-5

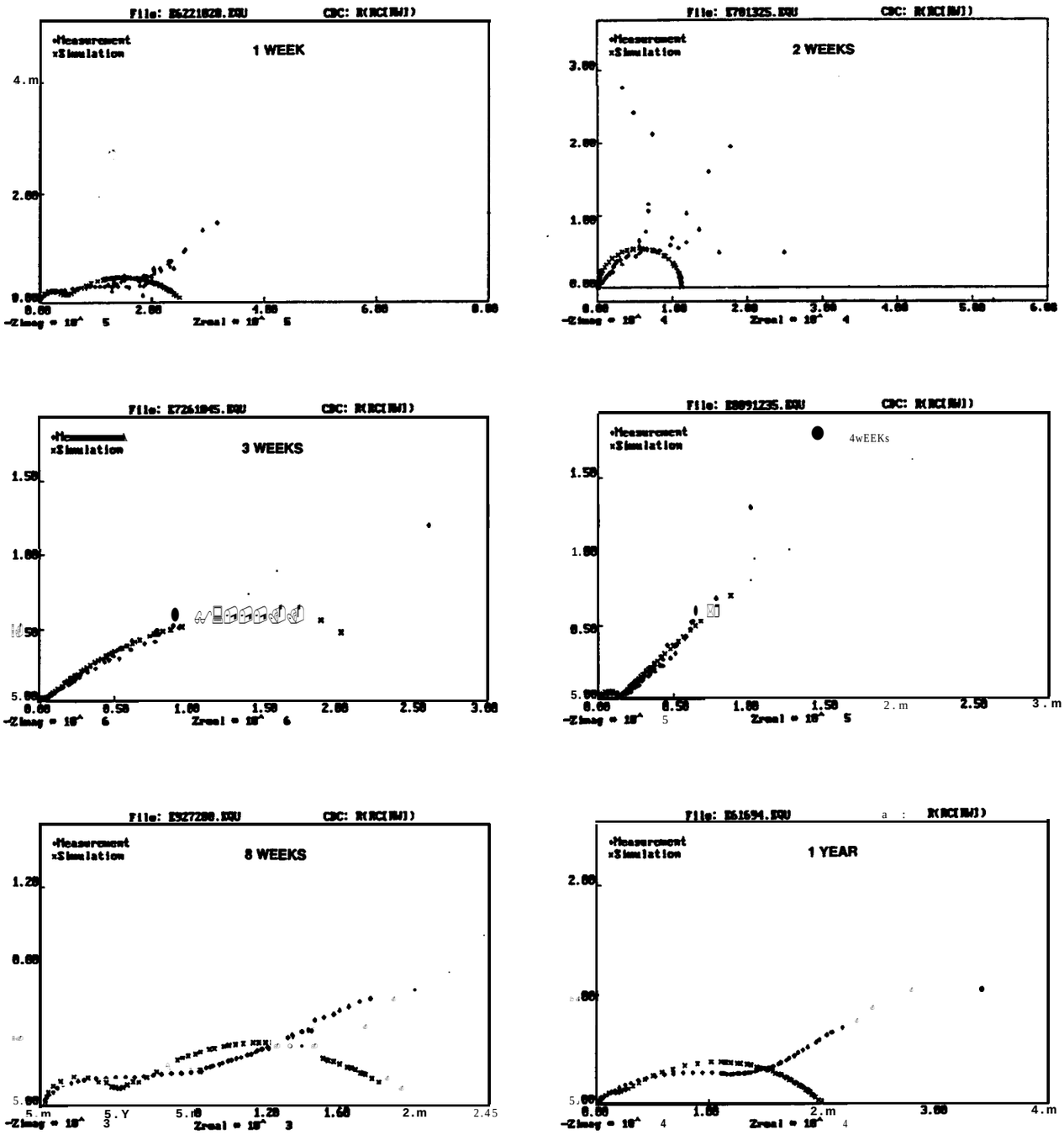

FIGUREA-10. NYQUISTPLOTSOFAMEROND-21-5

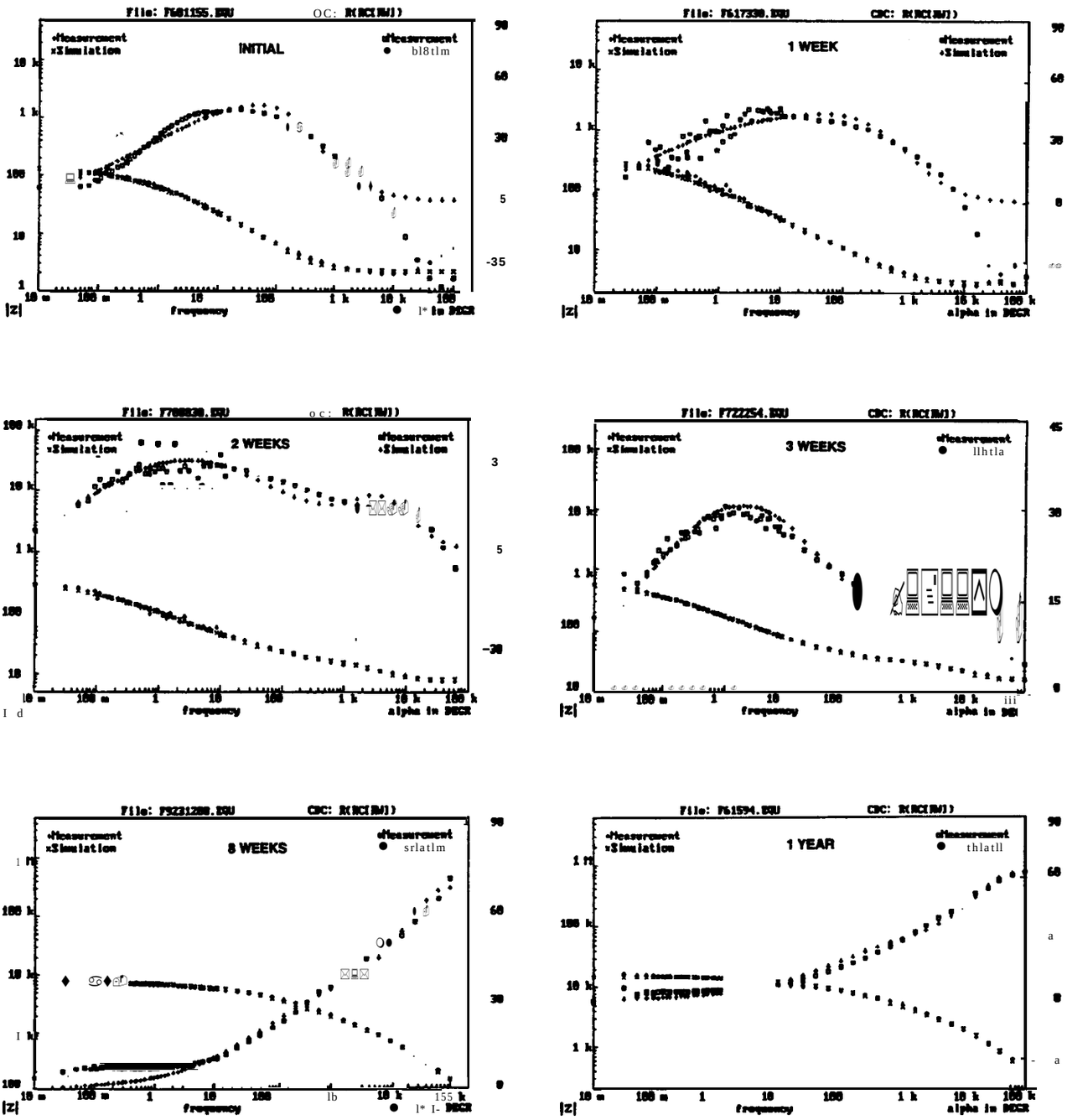

FIGURE A-11. BODE PLOTS OF BRINER V-65

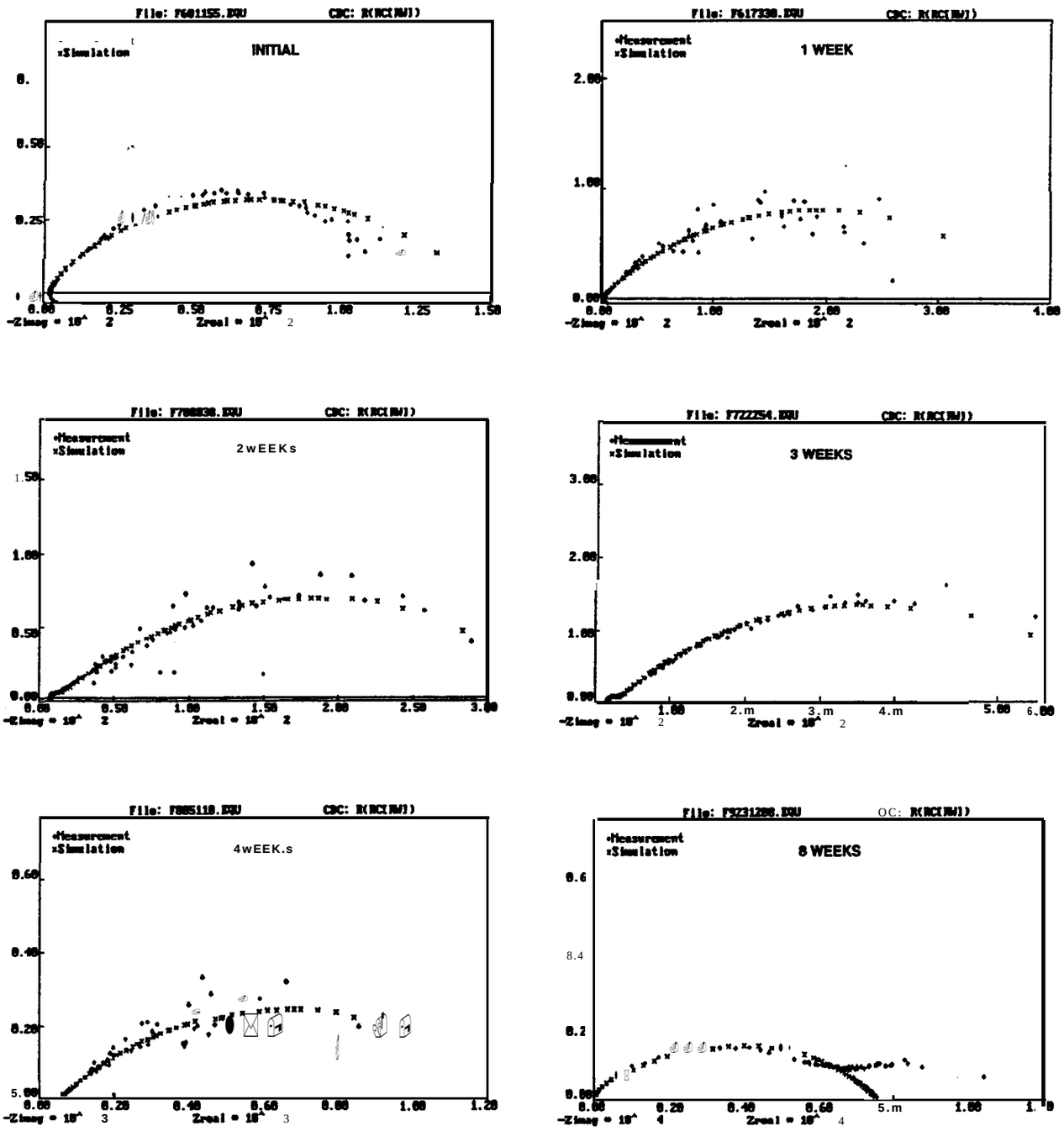

FIGURE A-12. NYQUISTPLOTS OFBRINERV-65

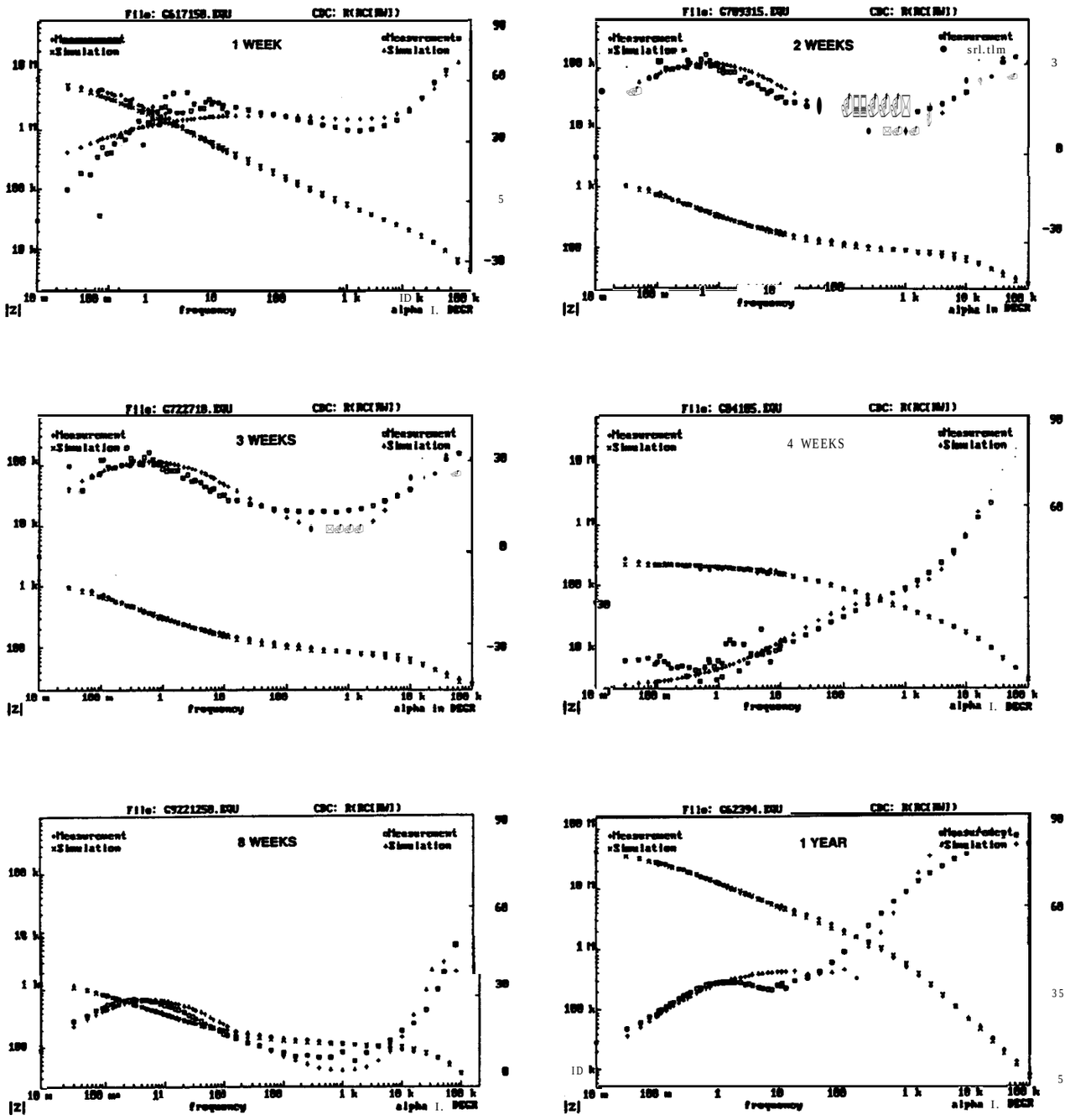

FIGURE A-13. BODE PLOTS FOR CARBOLINE CZ-D7

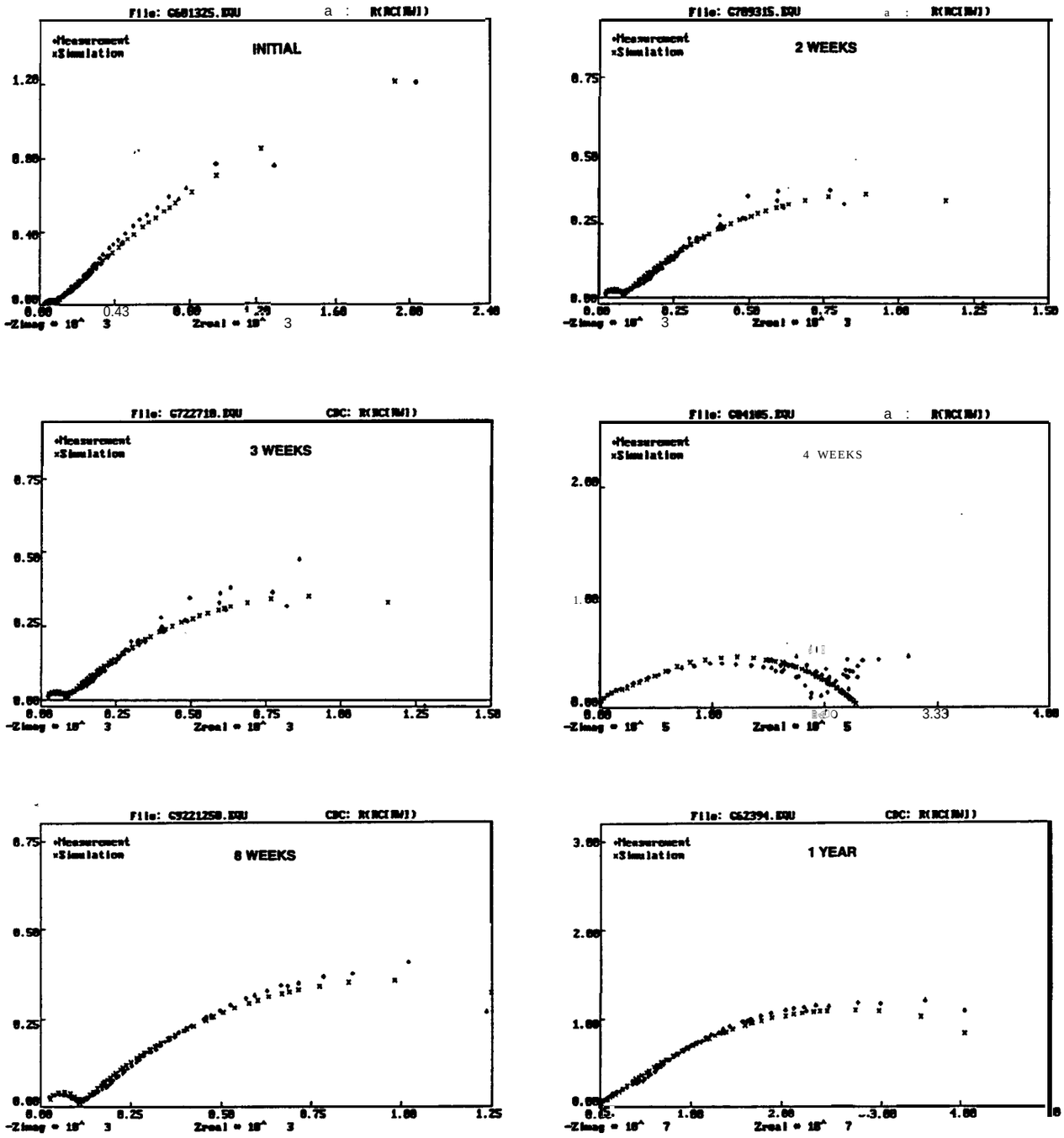

FIGURE A-14. NYQUIST PLOTS FOR CARBOLINE CZ-D7

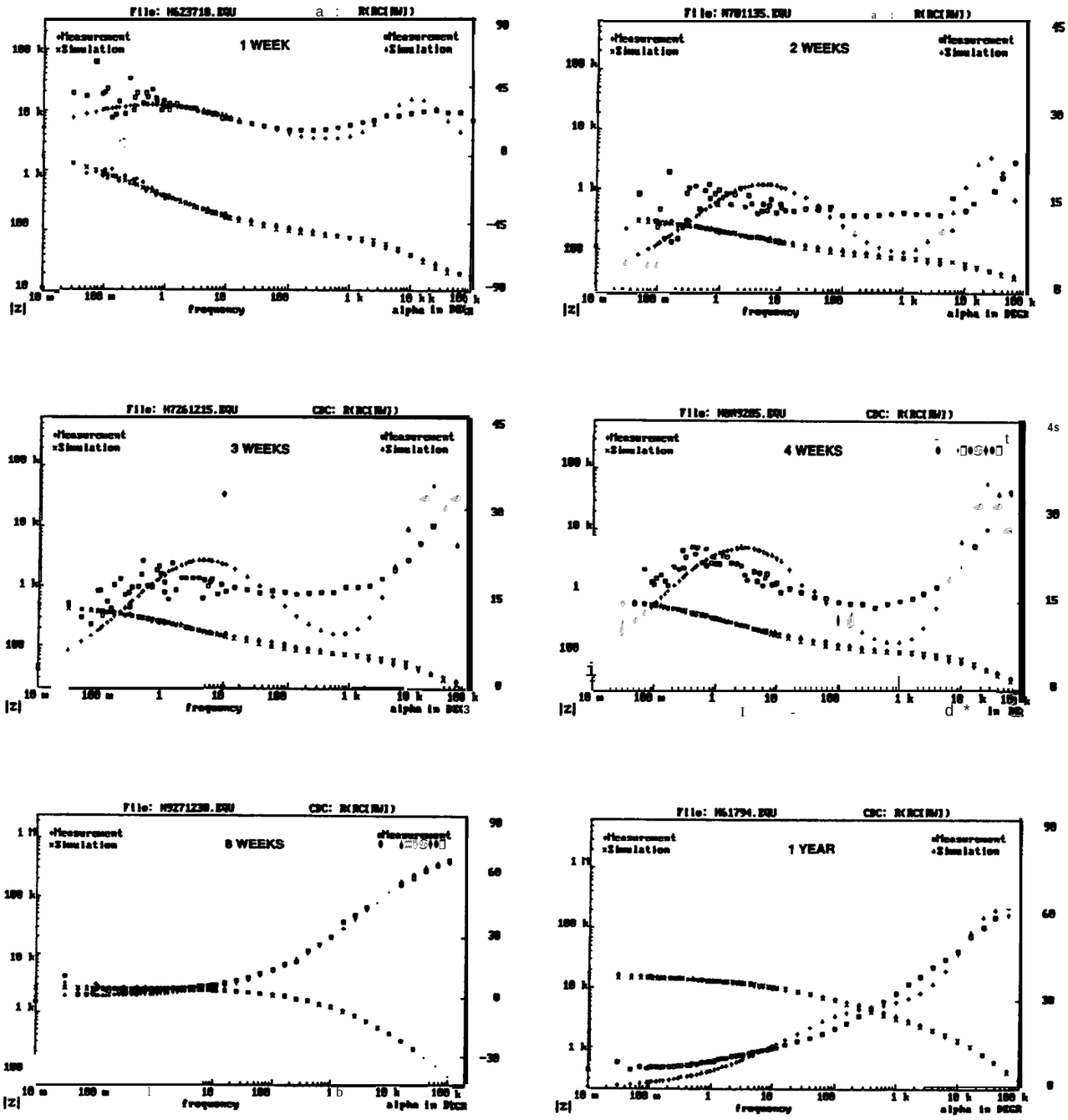

FIGURE A-15. BODE PLOTS OF DUPONT GANICIN 347 WB

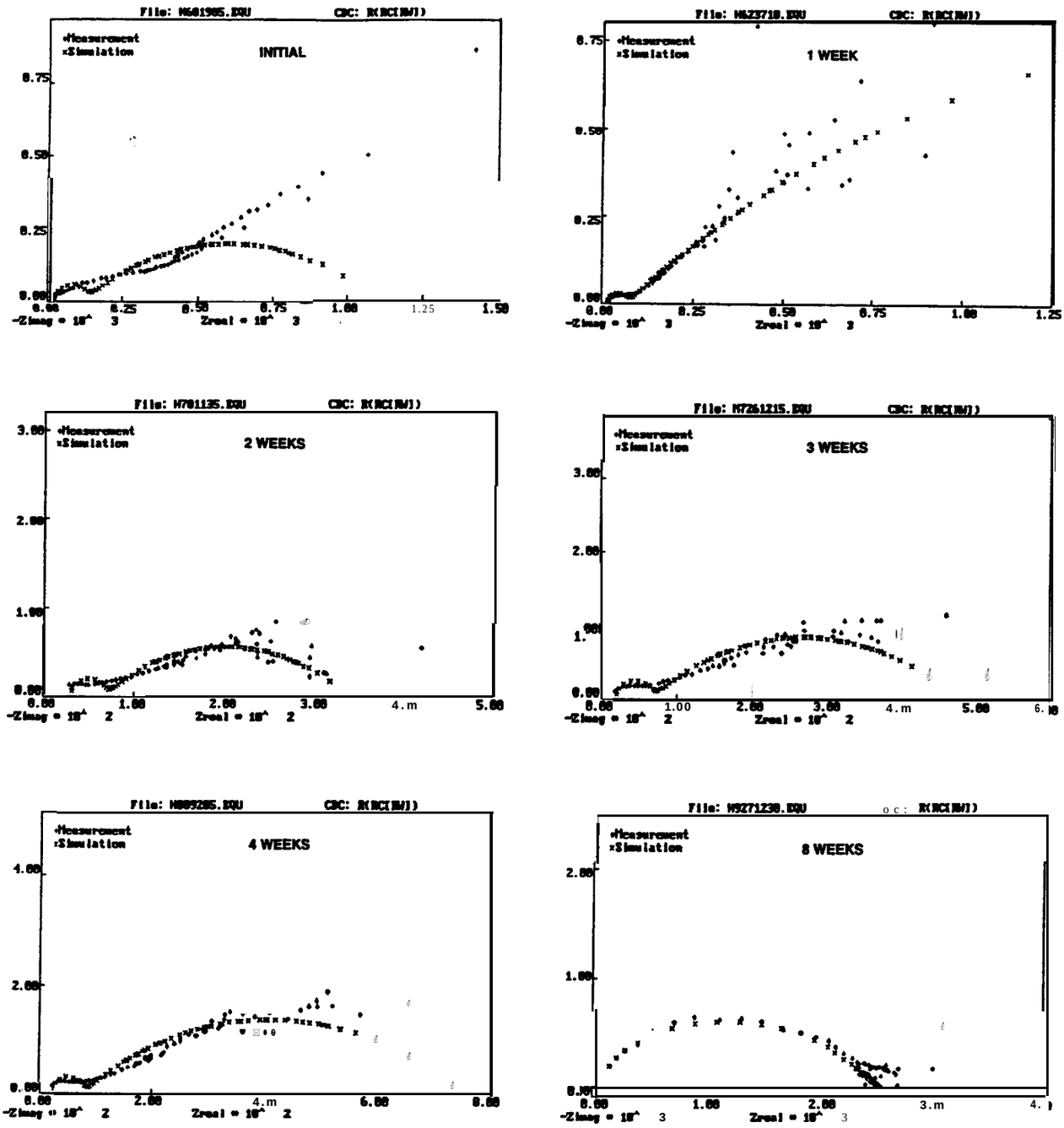

FIGURE A-16. NYQUIST PLOTS OF DUPONT GANICIN 347 WB

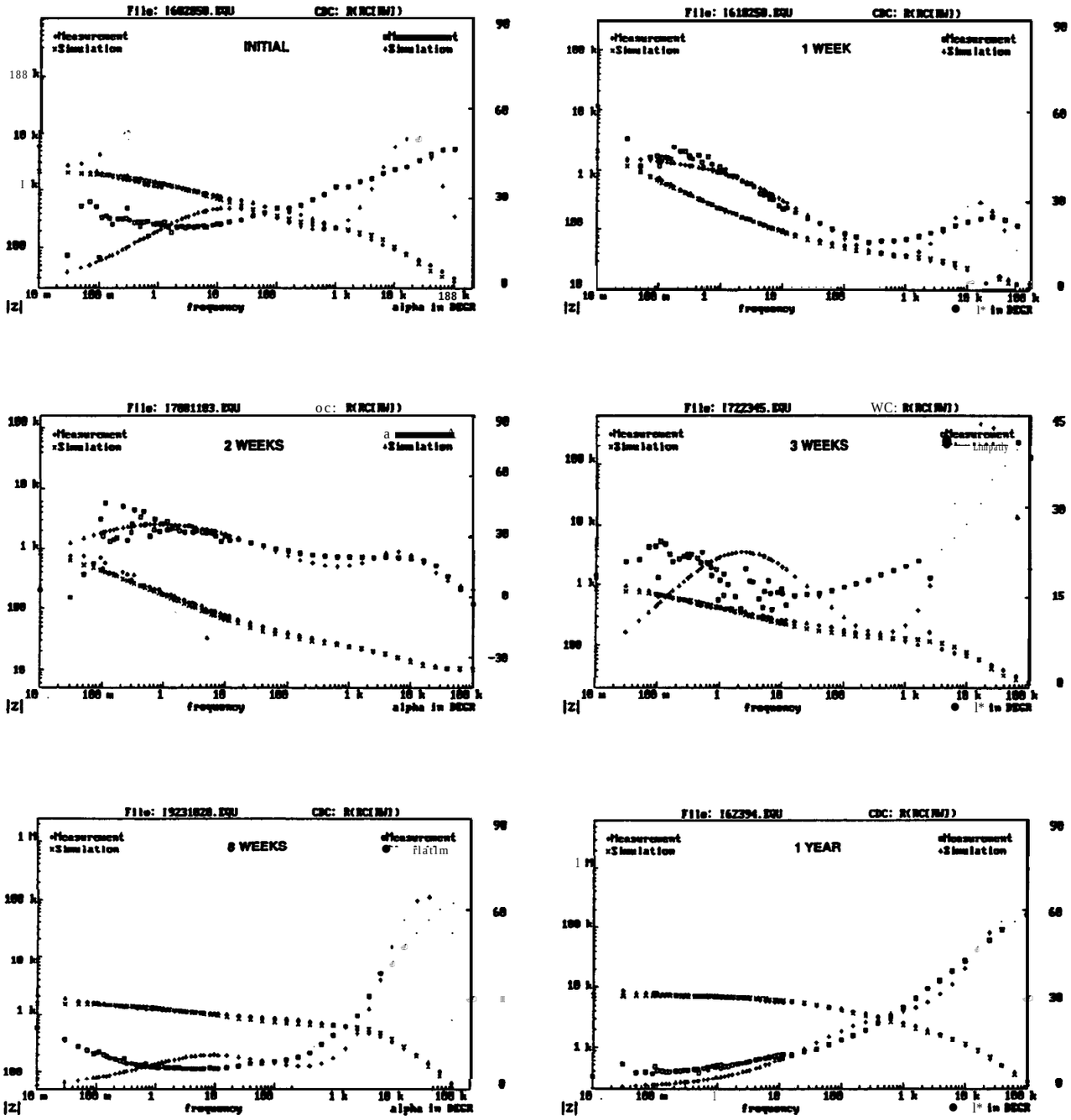

FIGURE A-17. BODE PLOTS OF INORGANIC COATINGS IC-531

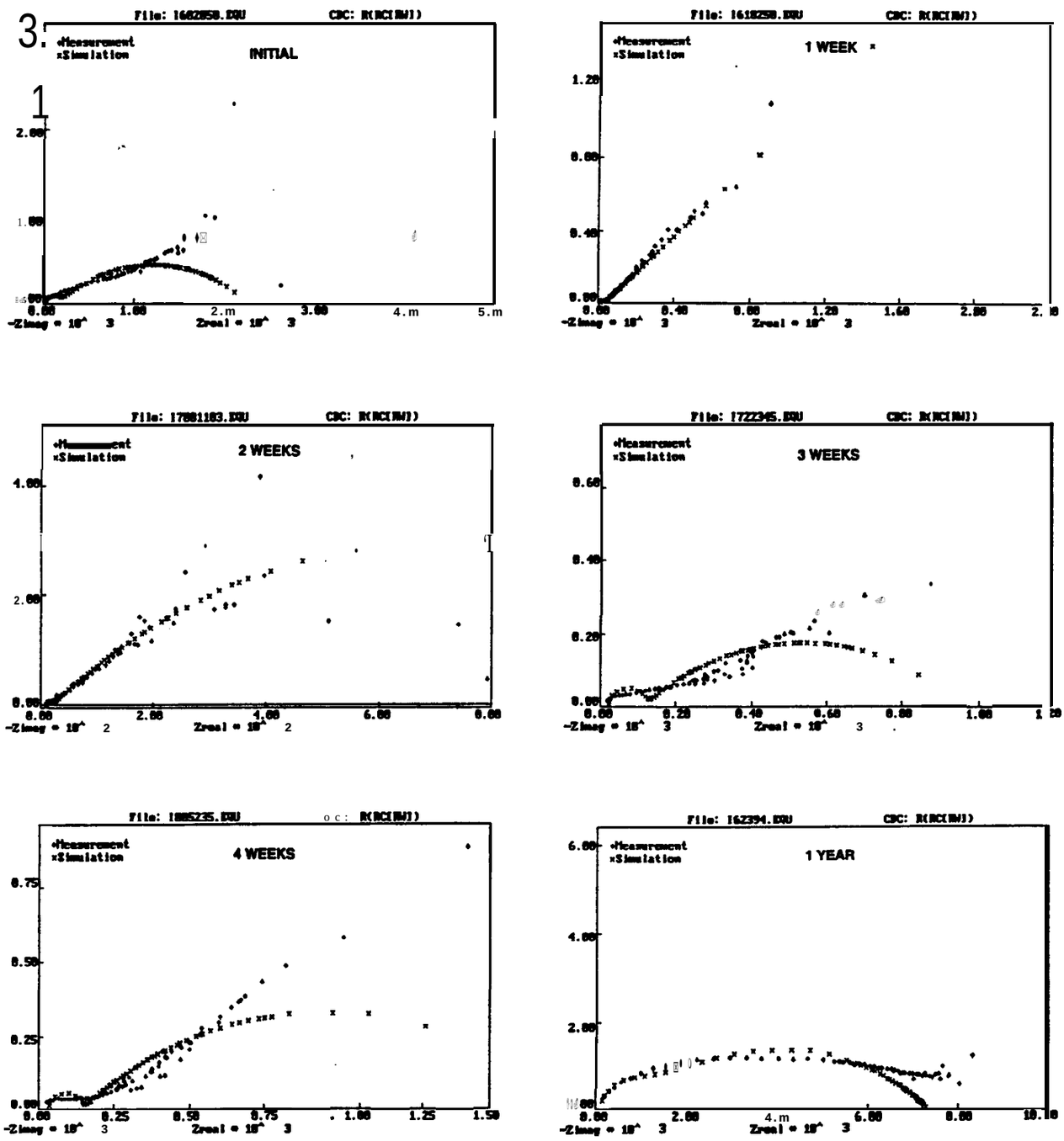

FIGURE A-18. NYQUIST PLOTS OF INORGANIC COATINGS IC-531

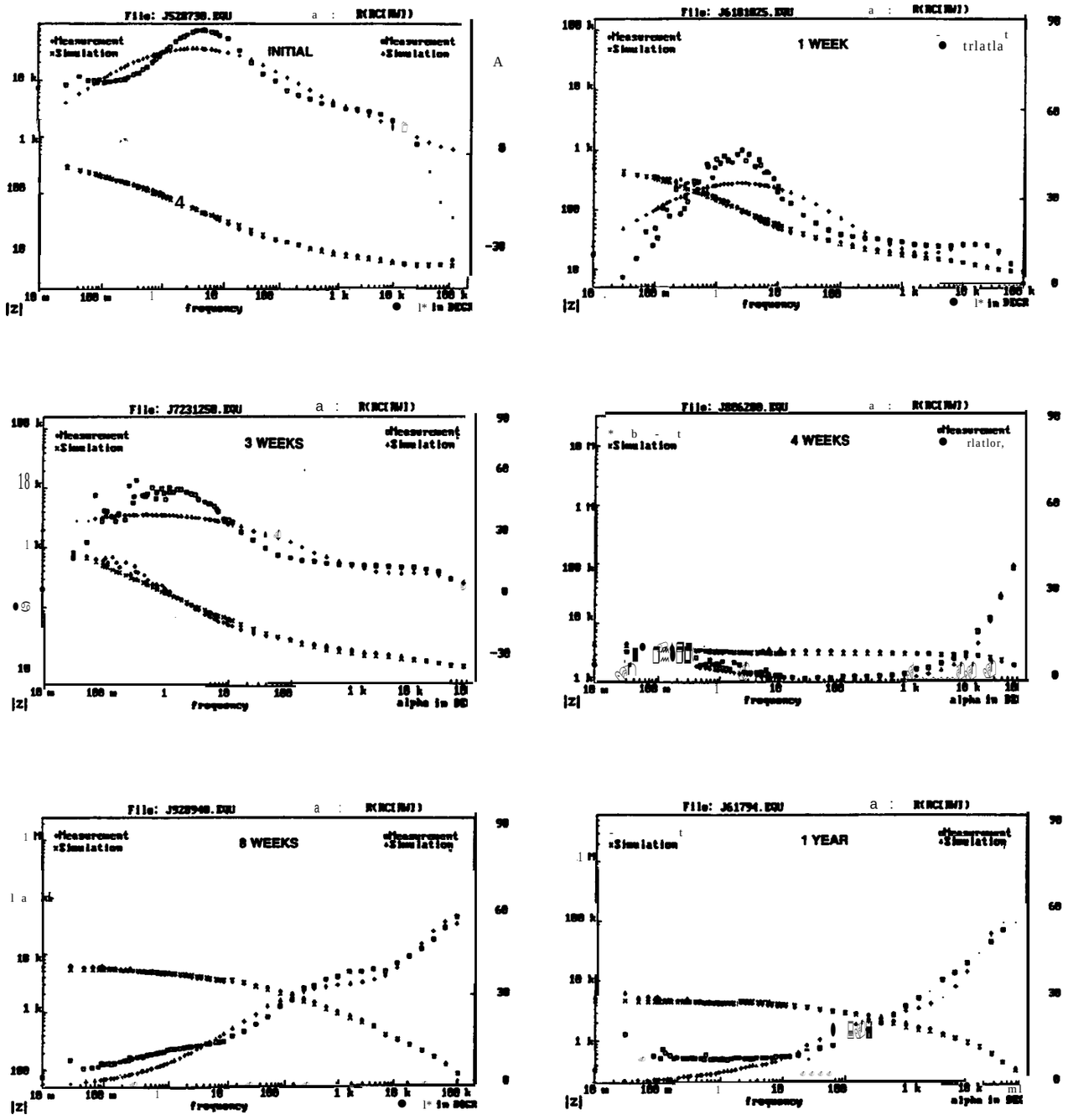

FIGURE A-19. BODE PLOTS OF PORTER TQ-4374H

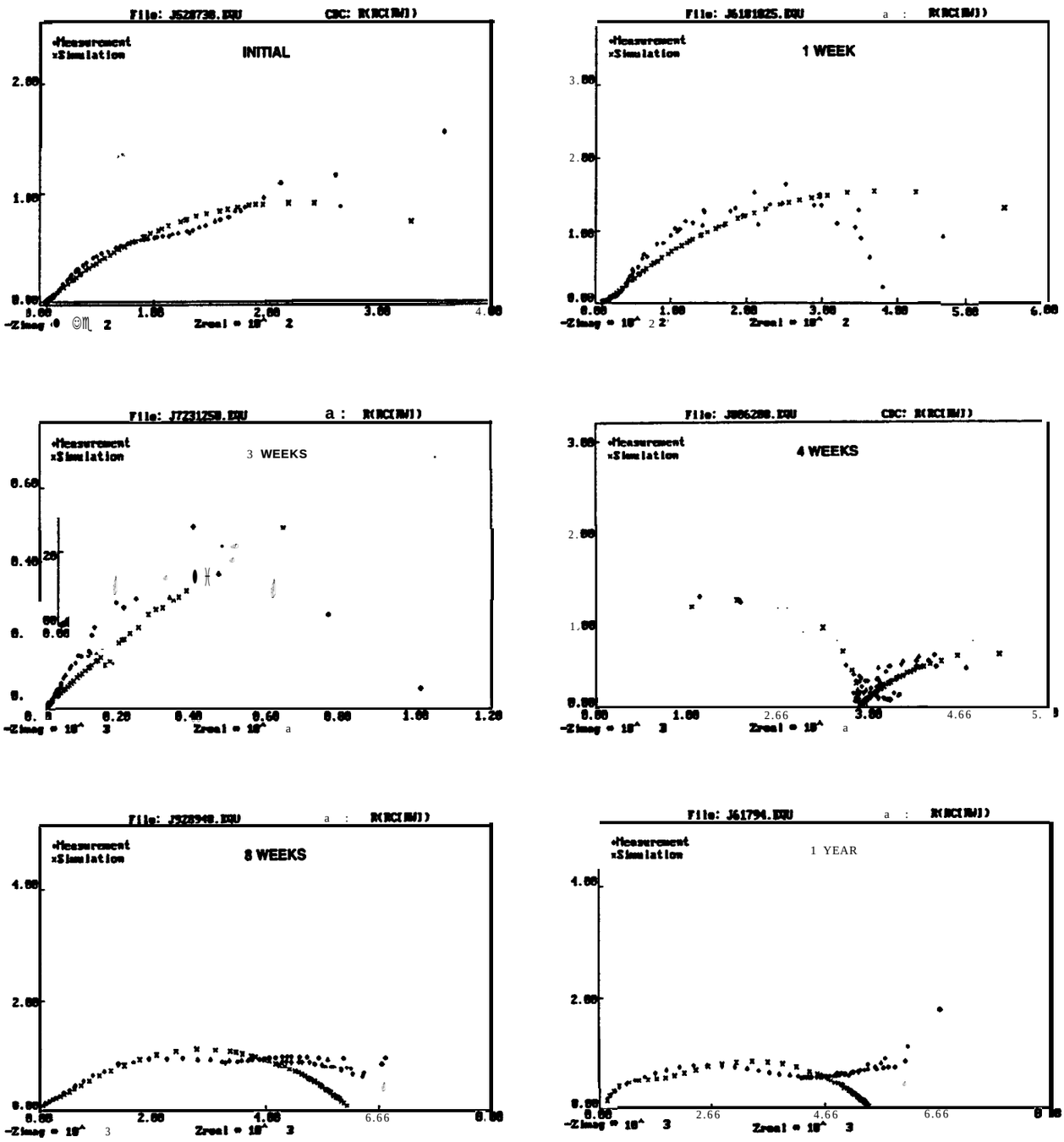

FIGURE A-20. NYQUIST PLOTS OF PORTER TQ-4374H

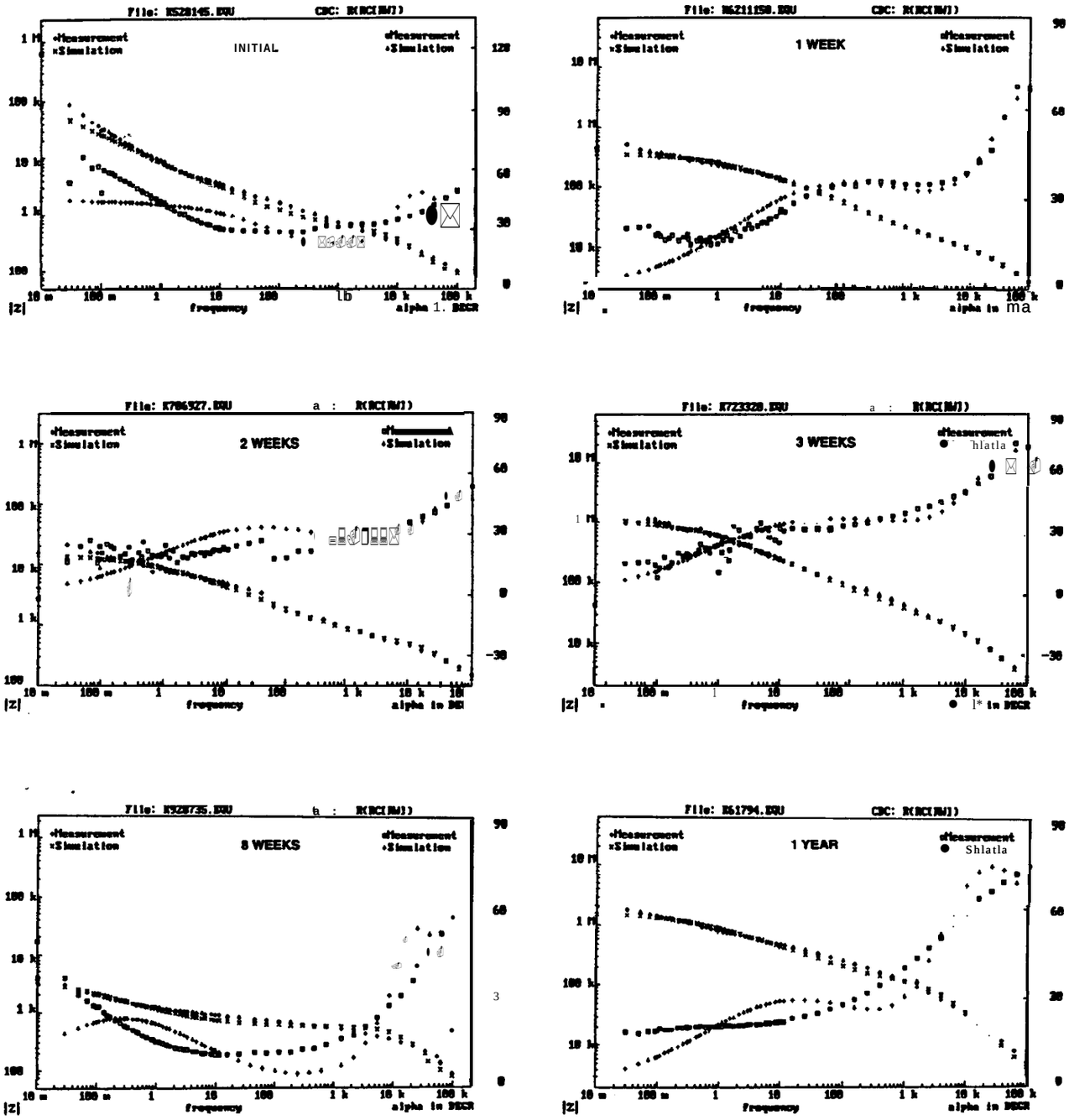

FIGURE A-21. BODEPLOTSOFSOUTHERNCOATINGSCHEMTEC600

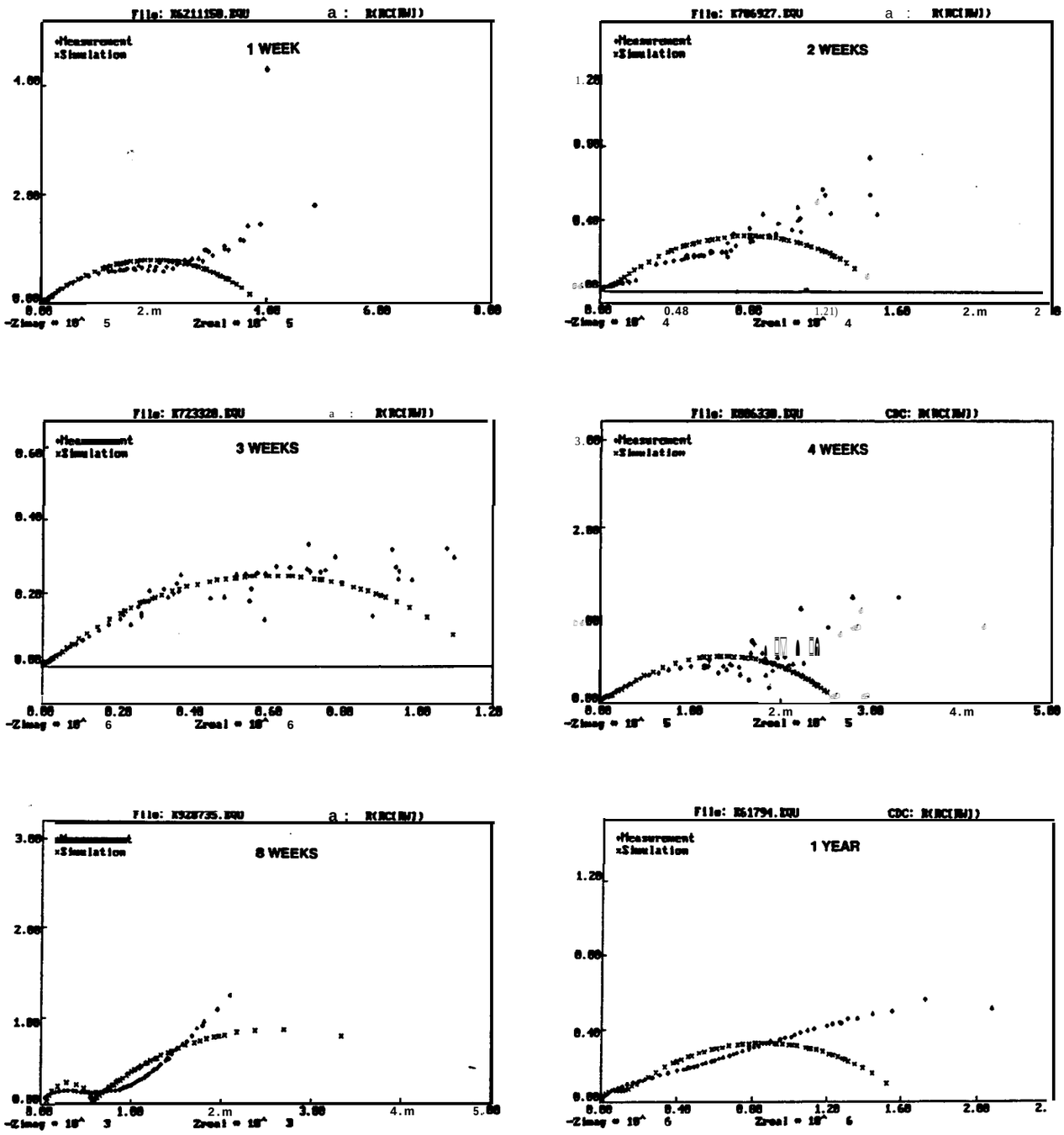

FIGUREA-22. NYQUISTPLOTSOFSOUTHERN COATINGS **CHEMTEC600**

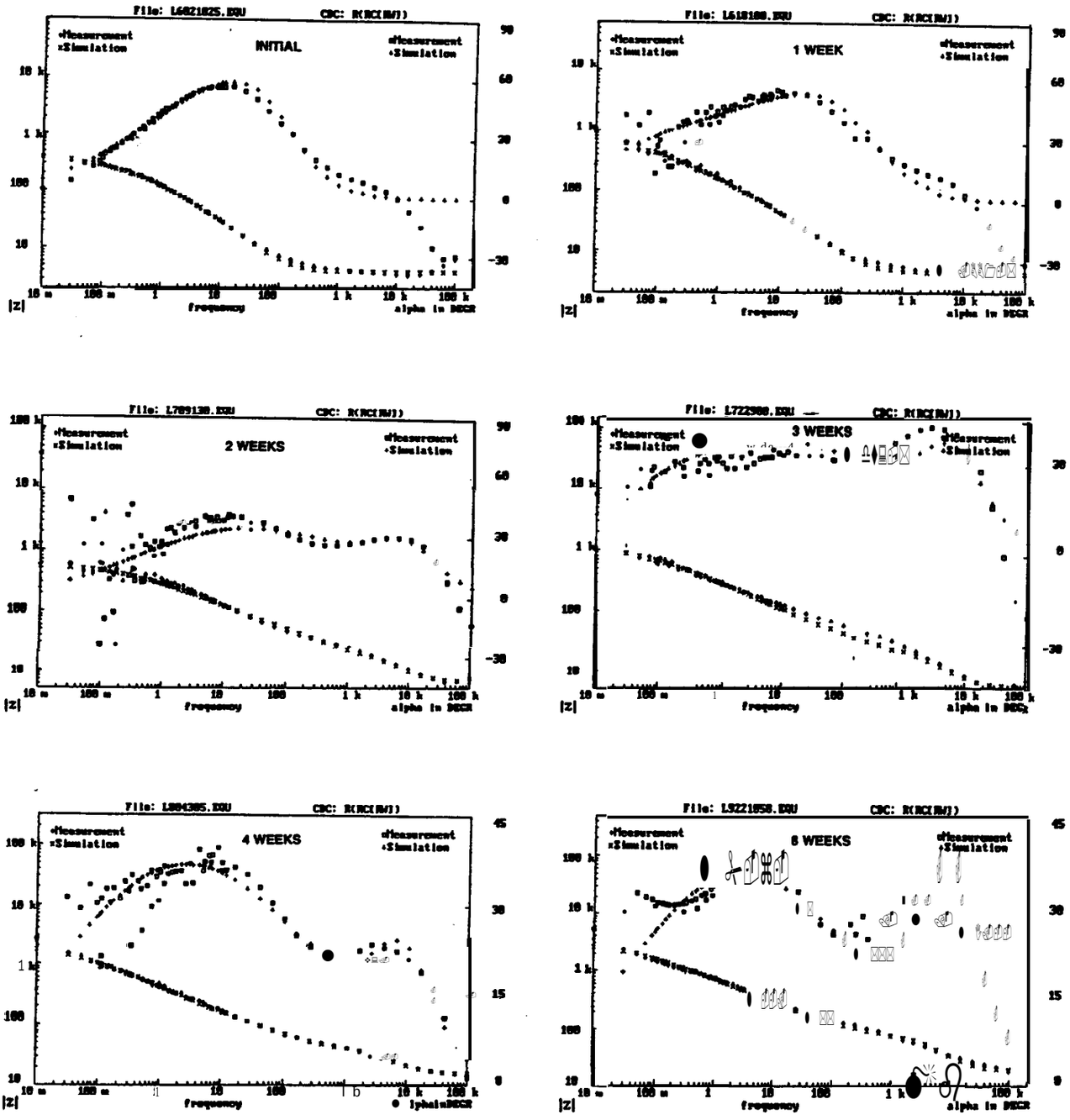

FIGUREA-23. BODEPLOTSOFSUBOXGALVANOXIV

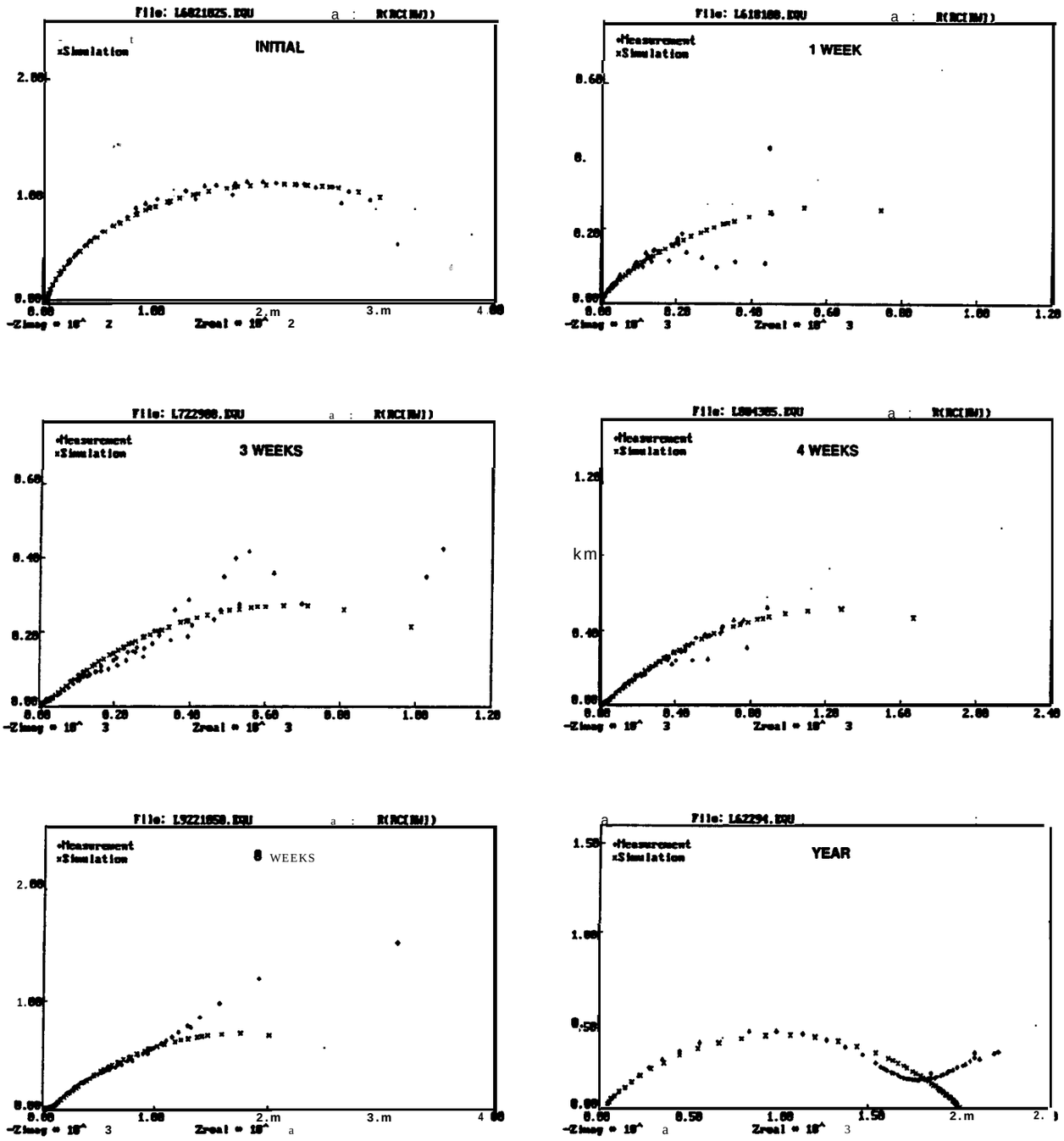

FIGURE A-24. NYQUIST PLOTS OF SUBOX GALVANOX IV

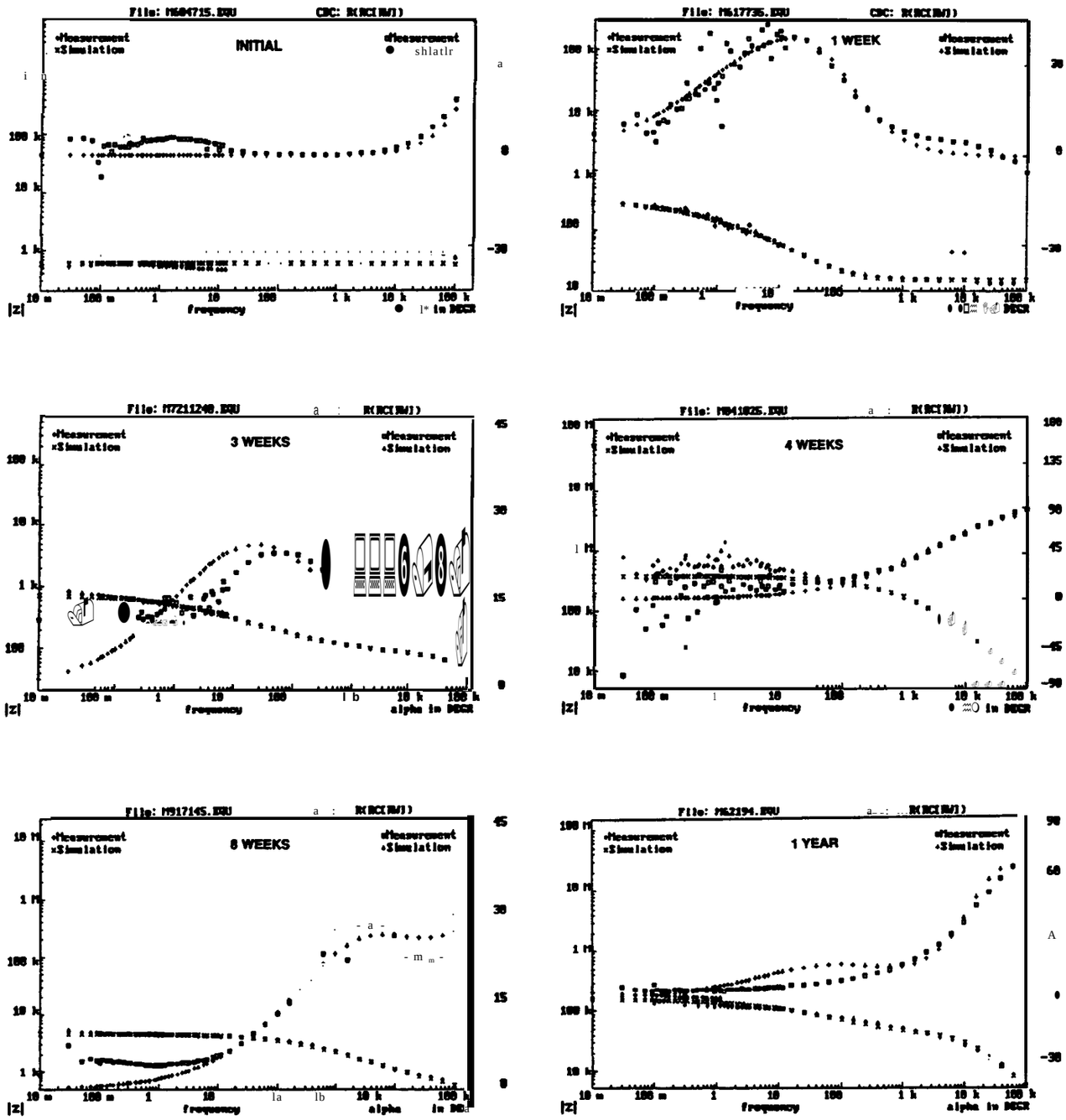

FIGURE A-25. BODEPLOTSOFBYCOSP-101

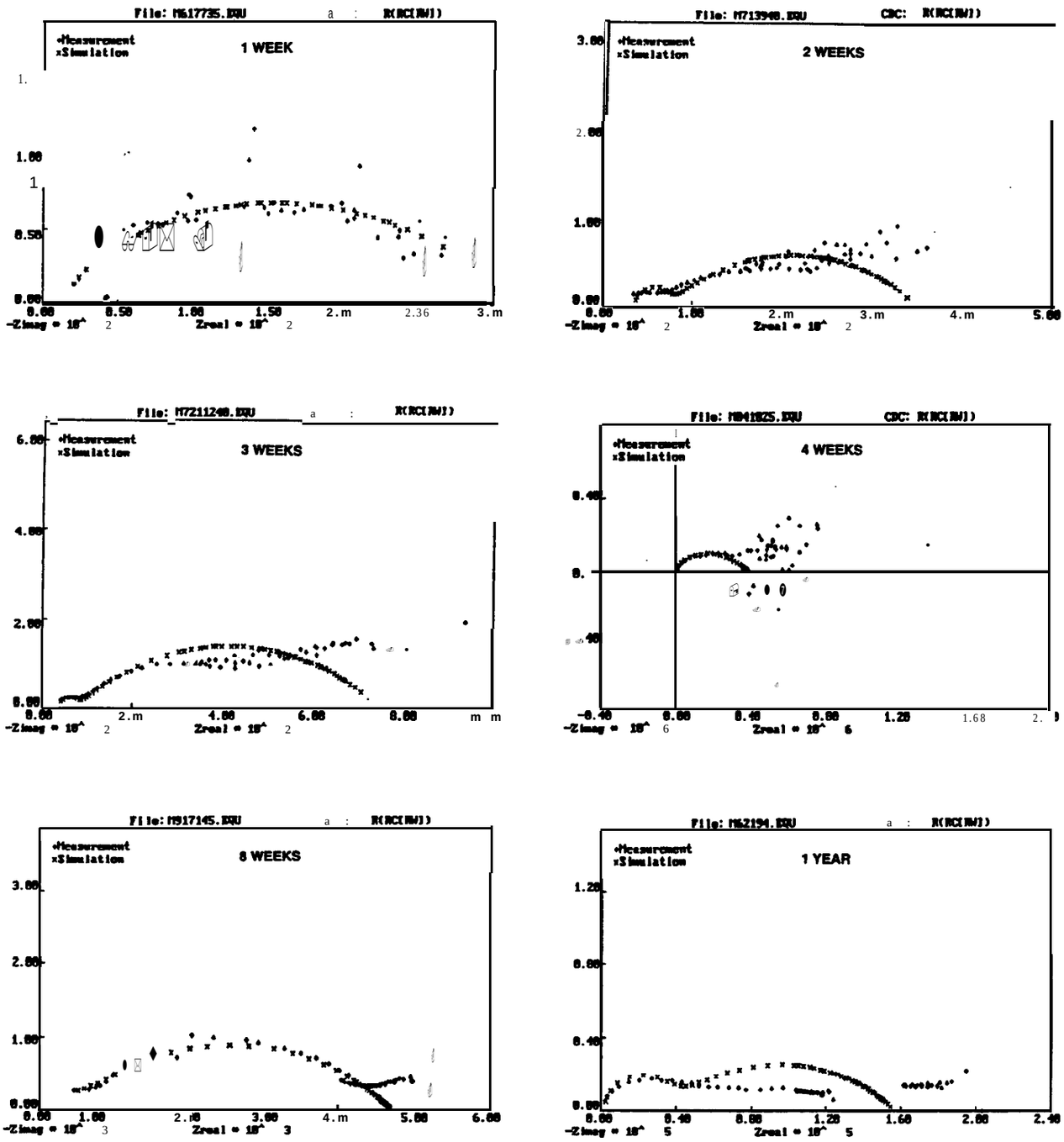

FIGUREA-26. NYQUISTPLOTSOFBYCO SP-101

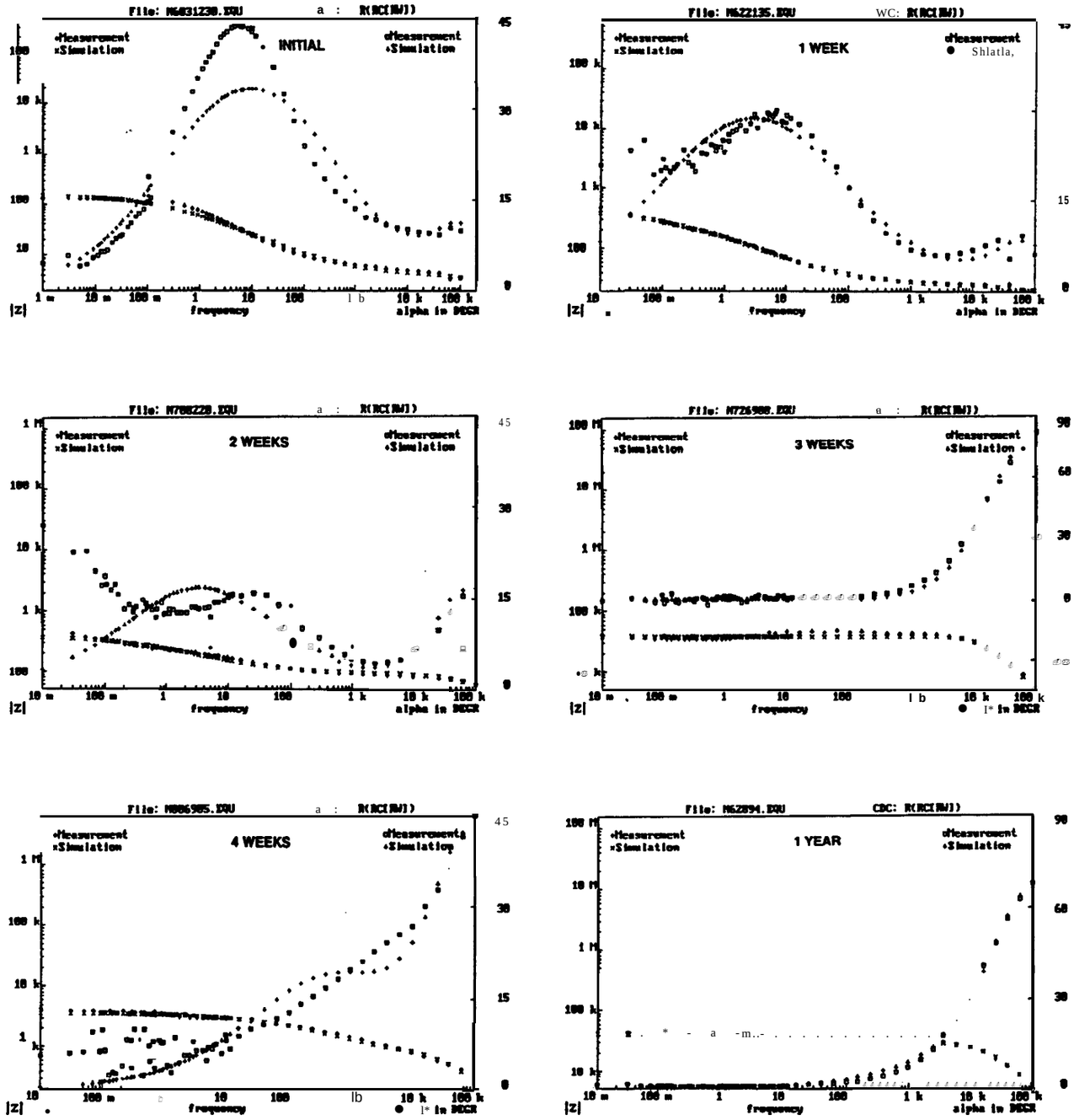

FIGUREA-27. BODE PLOTS OF CARBOLINE CZ-11

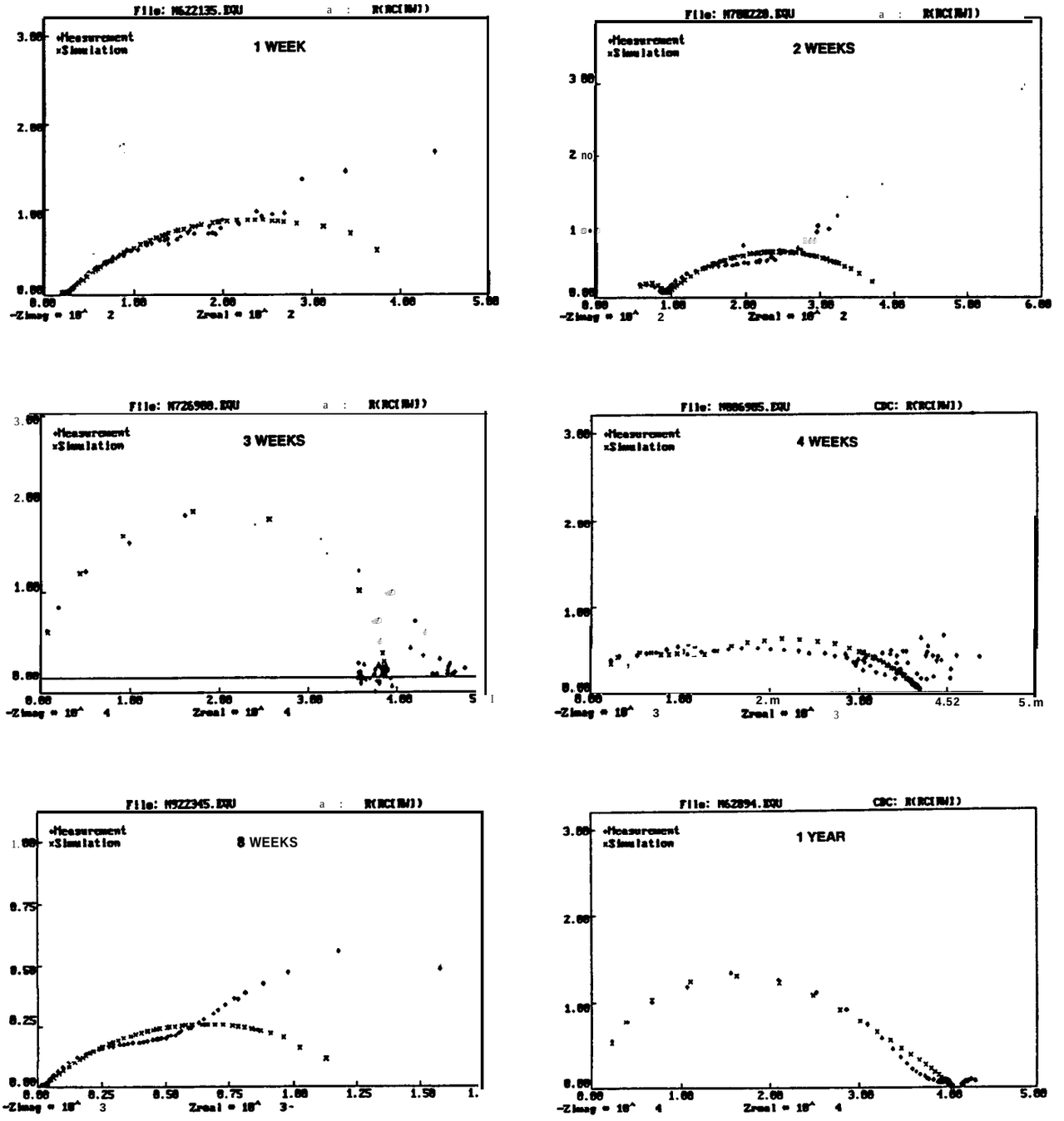

FIGURE A-28. NYQUIST PLOTS OF CARBOLINE CZ-11

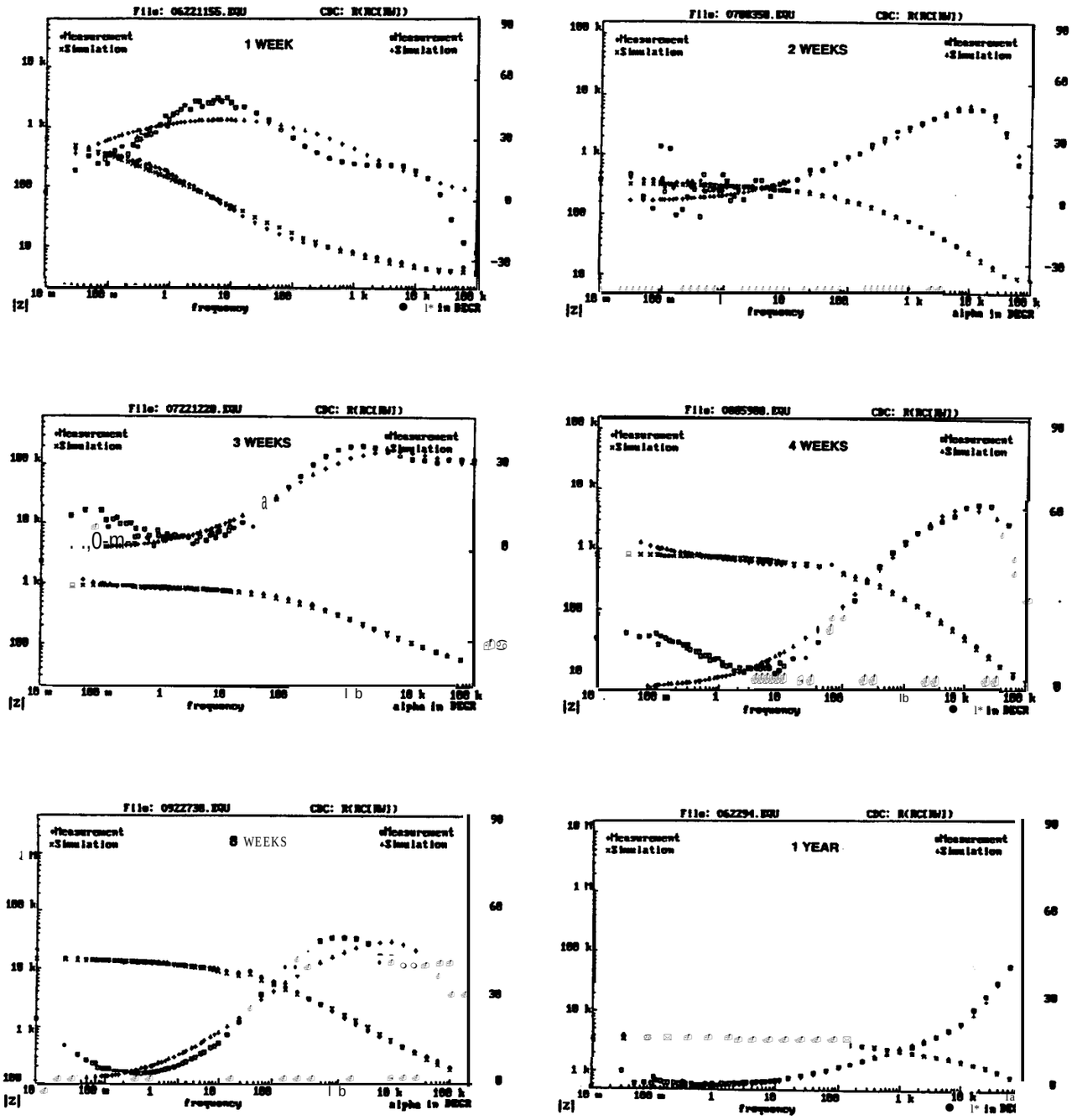

FIGUREA-29. BODE PLOTS OF CORONADO 935-152

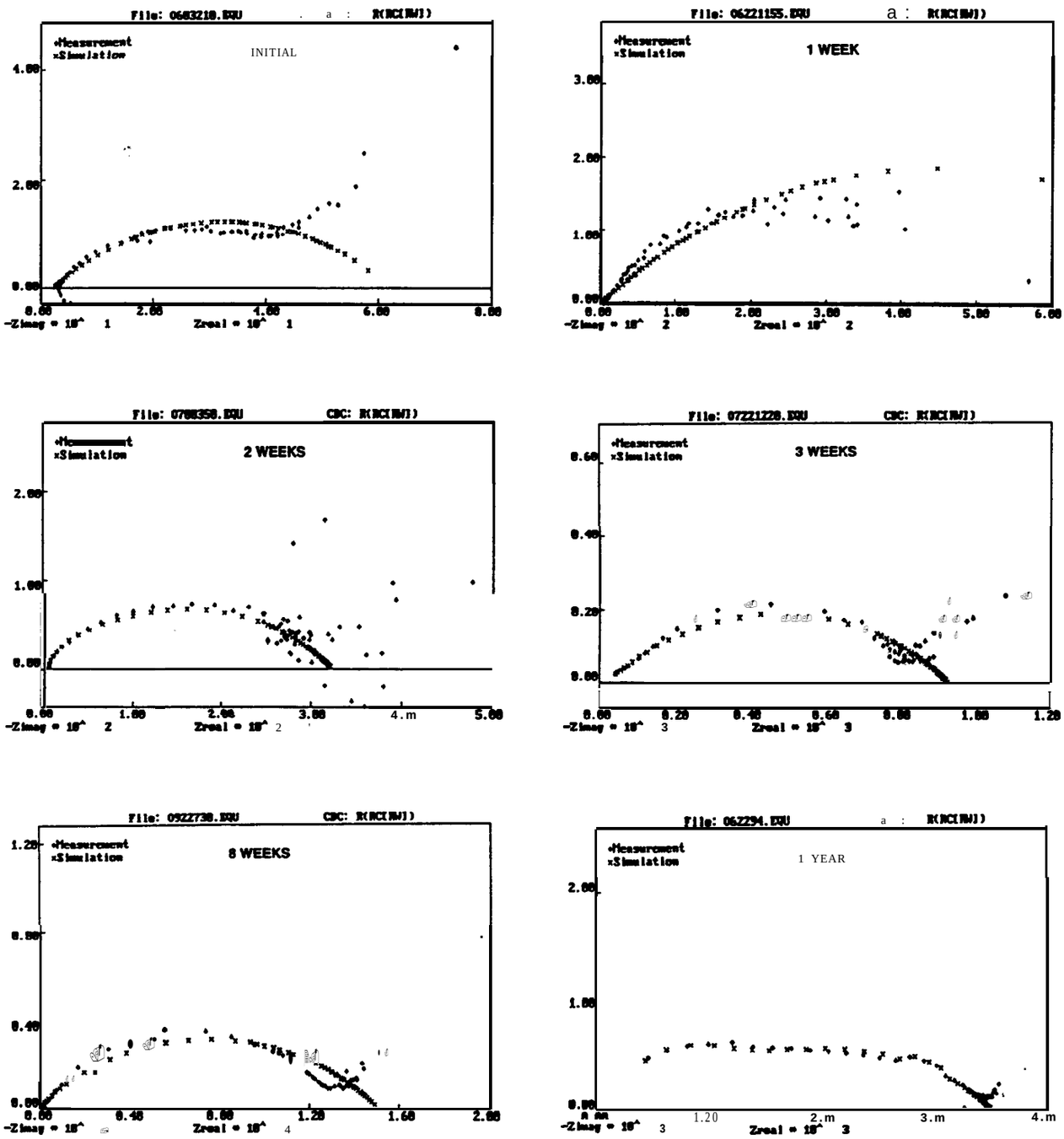

FIGURE A-30. NYQUIST PLOTS OF CORONADO 935-152

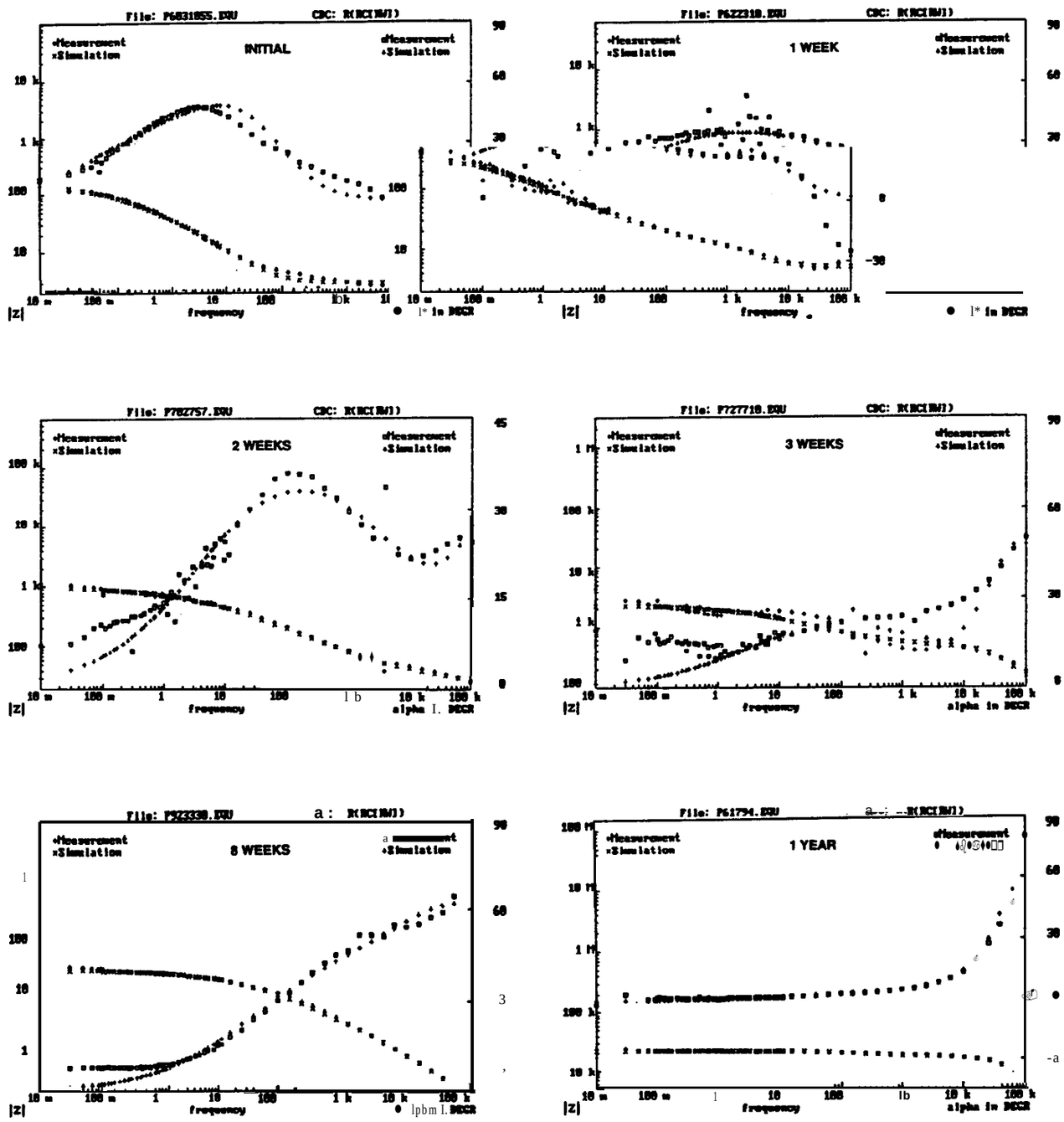

FIGURE A-31. BODEPLOTSOFDEVOECATHA-COAT304

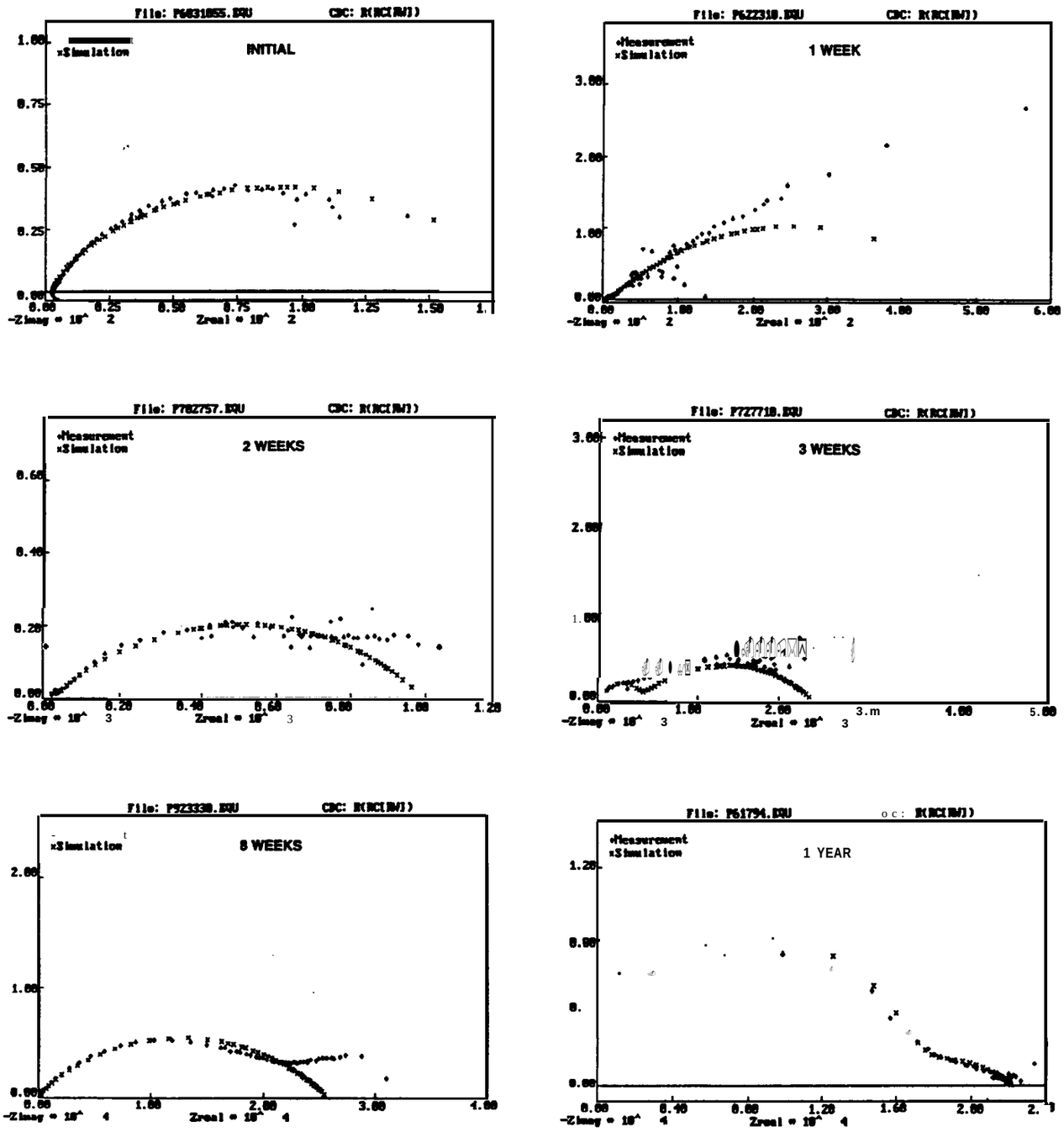

FIGURE A-32. NYQUIST PLOTS OF DEVOE CATHA-COAT 304

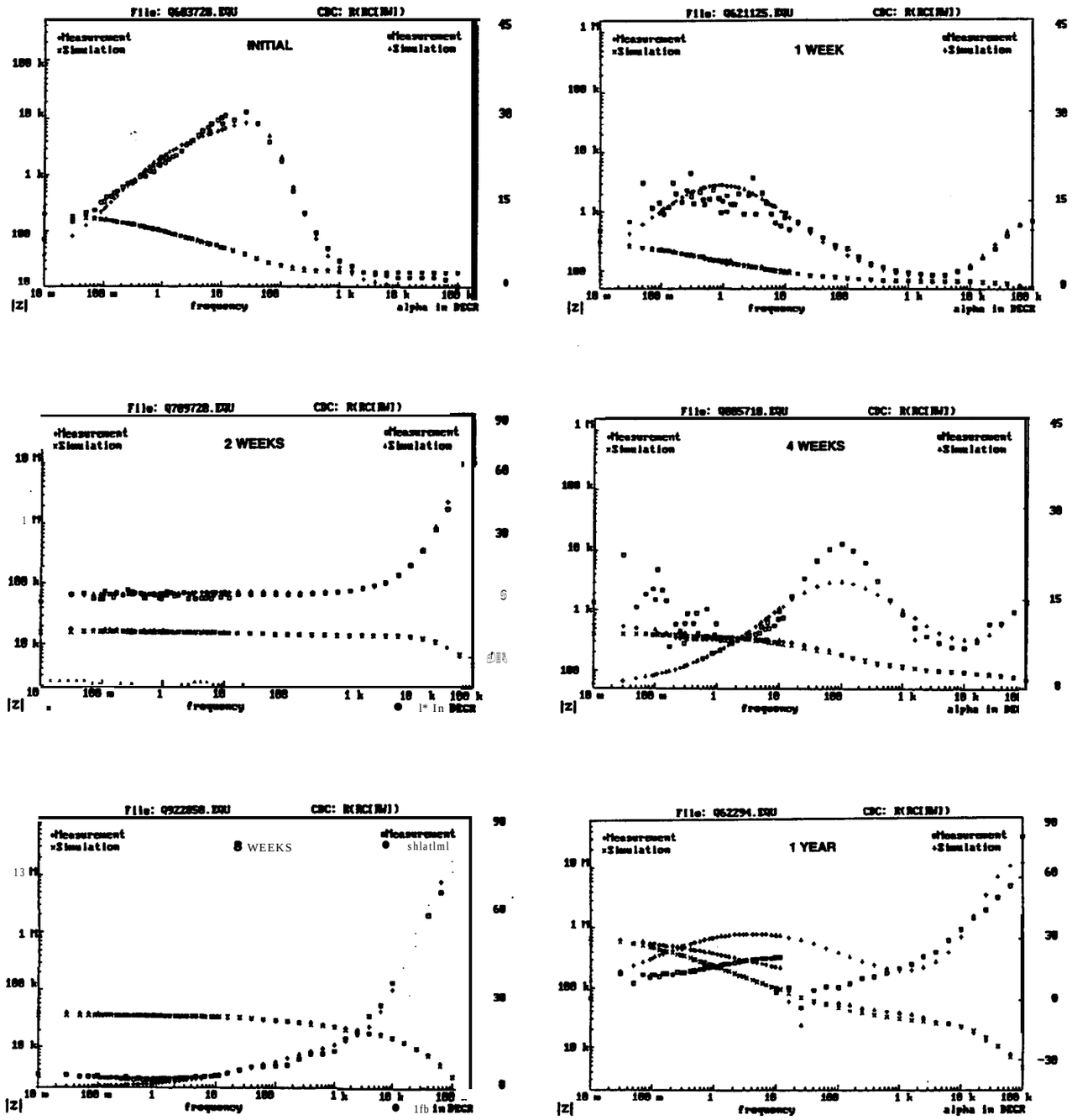

FIGURE A-33. BODE PLOTS OF GLIDDEN GLID-ZINC 5530

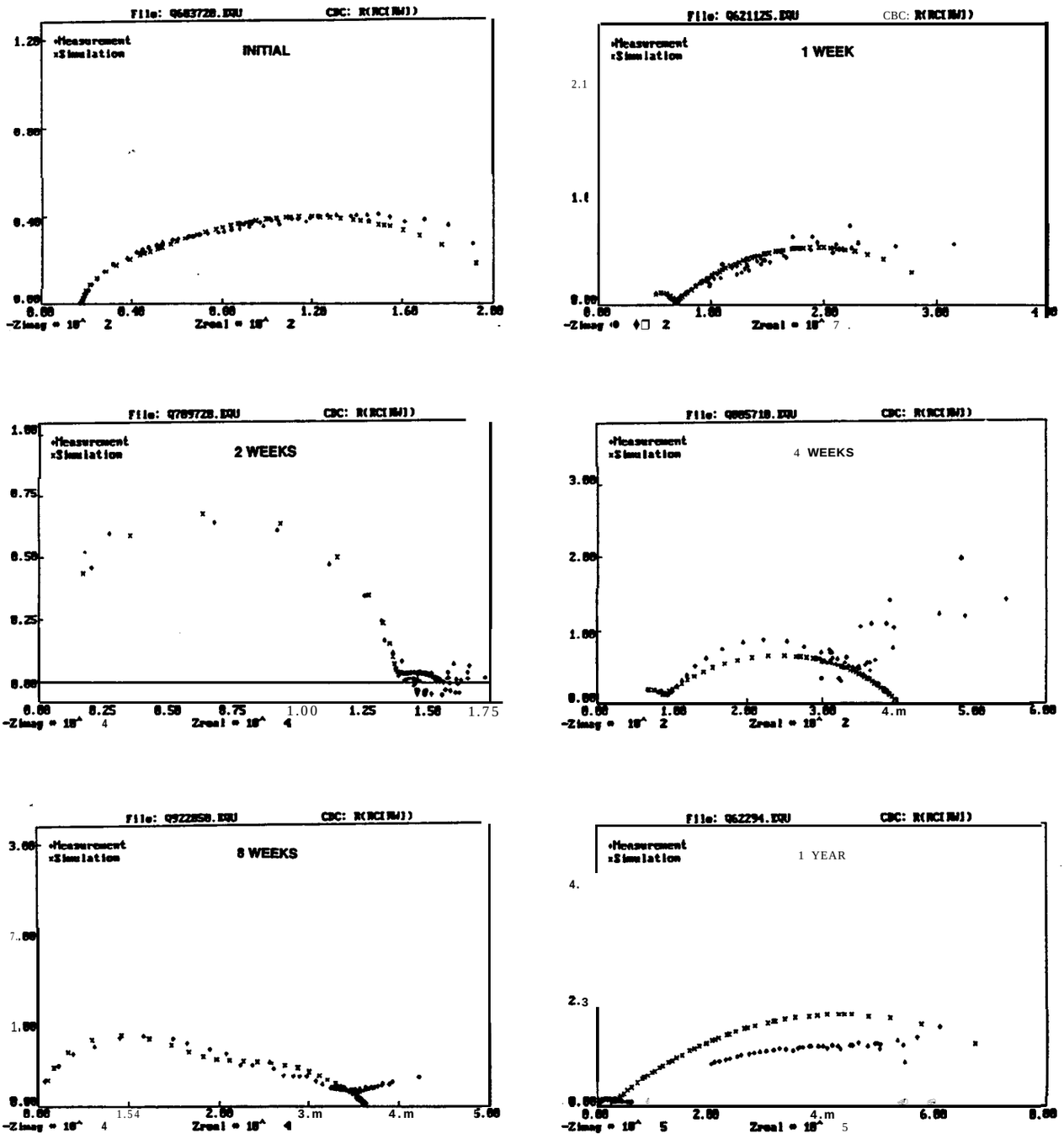

FIGURE A-34. NYQUIST PLOTS OF GLIDDEN GLID-ZINC 5530

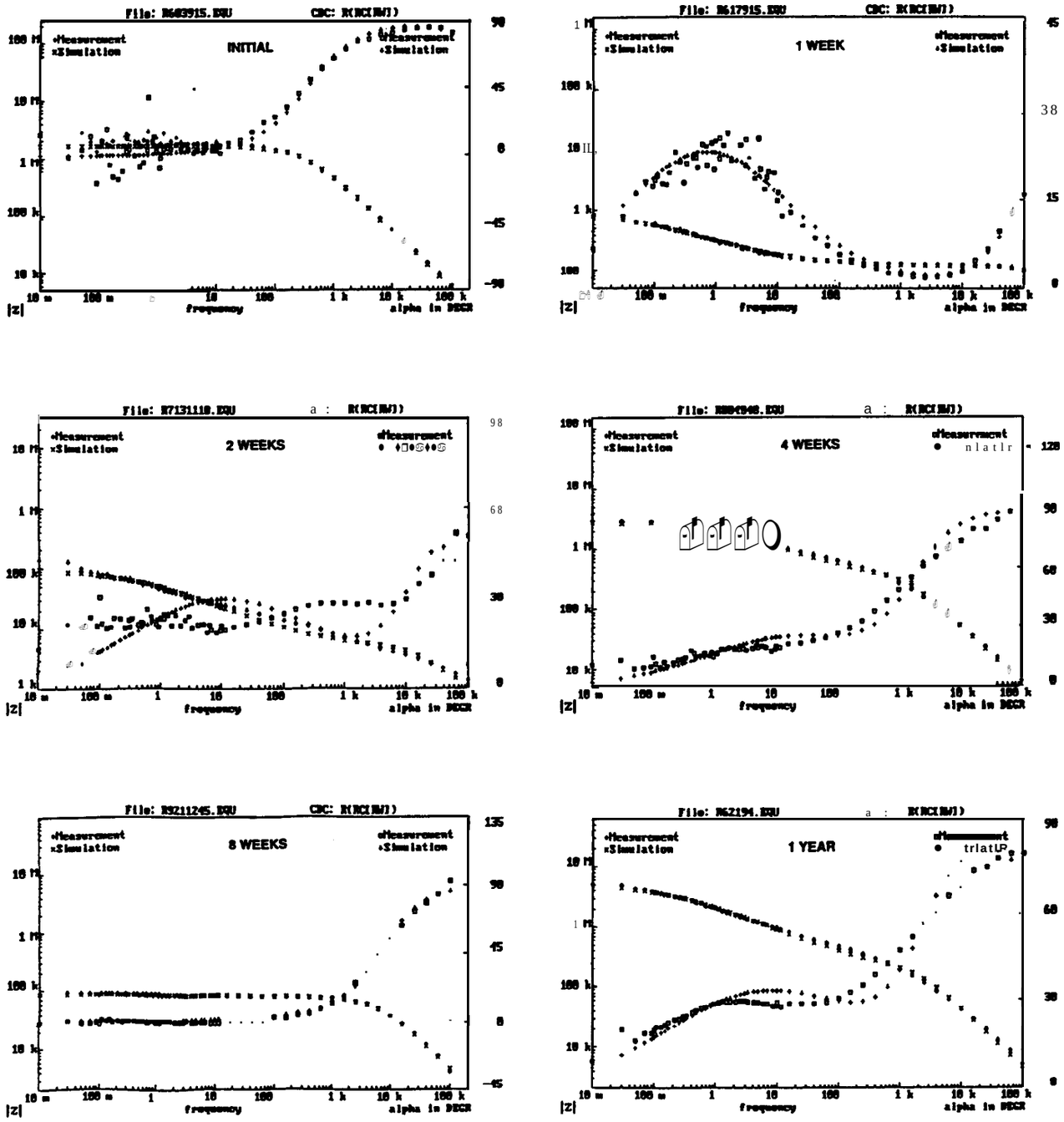

FIGURE A-35. BODE PLOTS OF GLIDDEN GLID-ZINC 5536

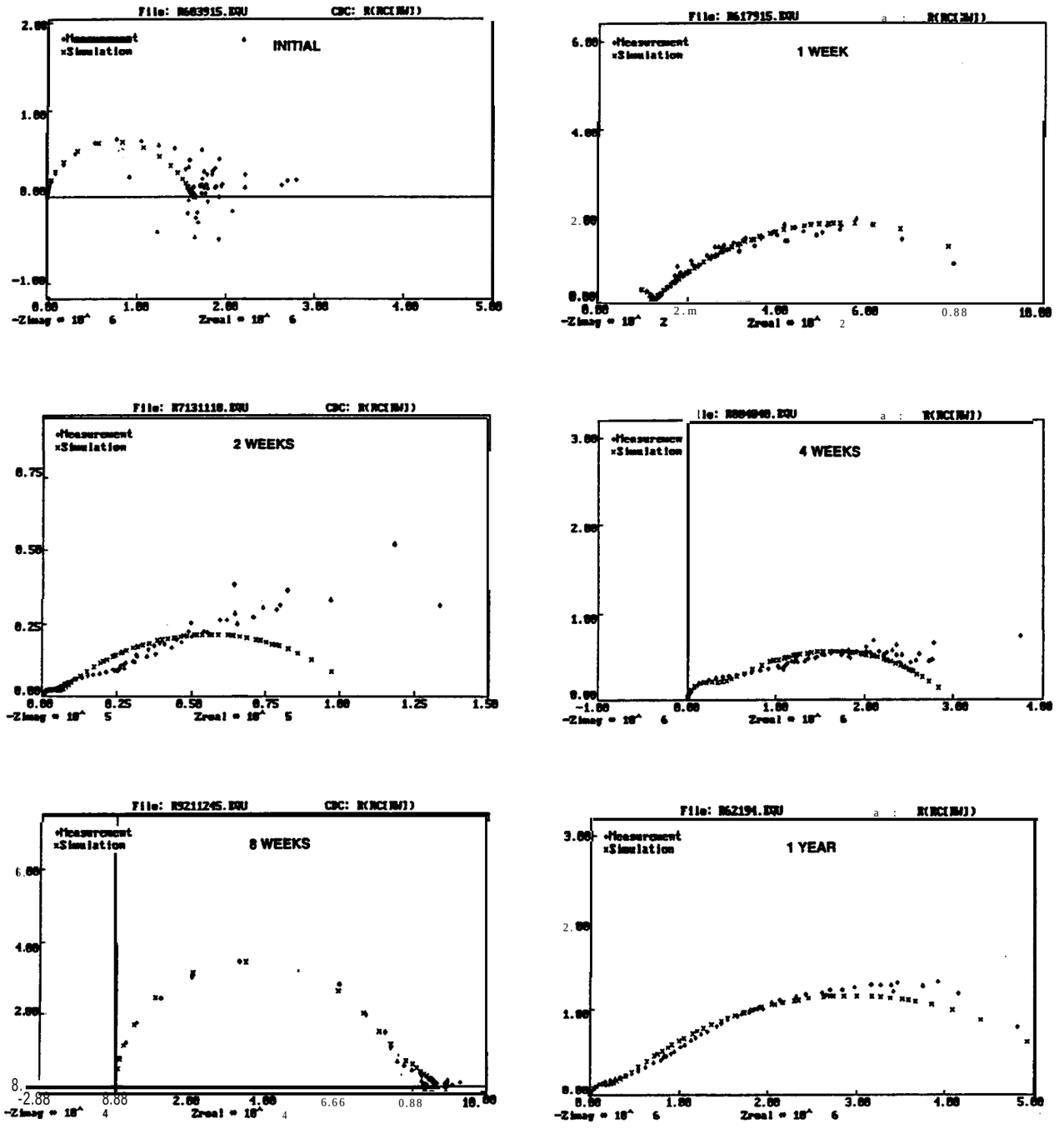

FIGURE A-36. NYQUIST PLOTS OF GLIDDEN GLID-ZINC 5536

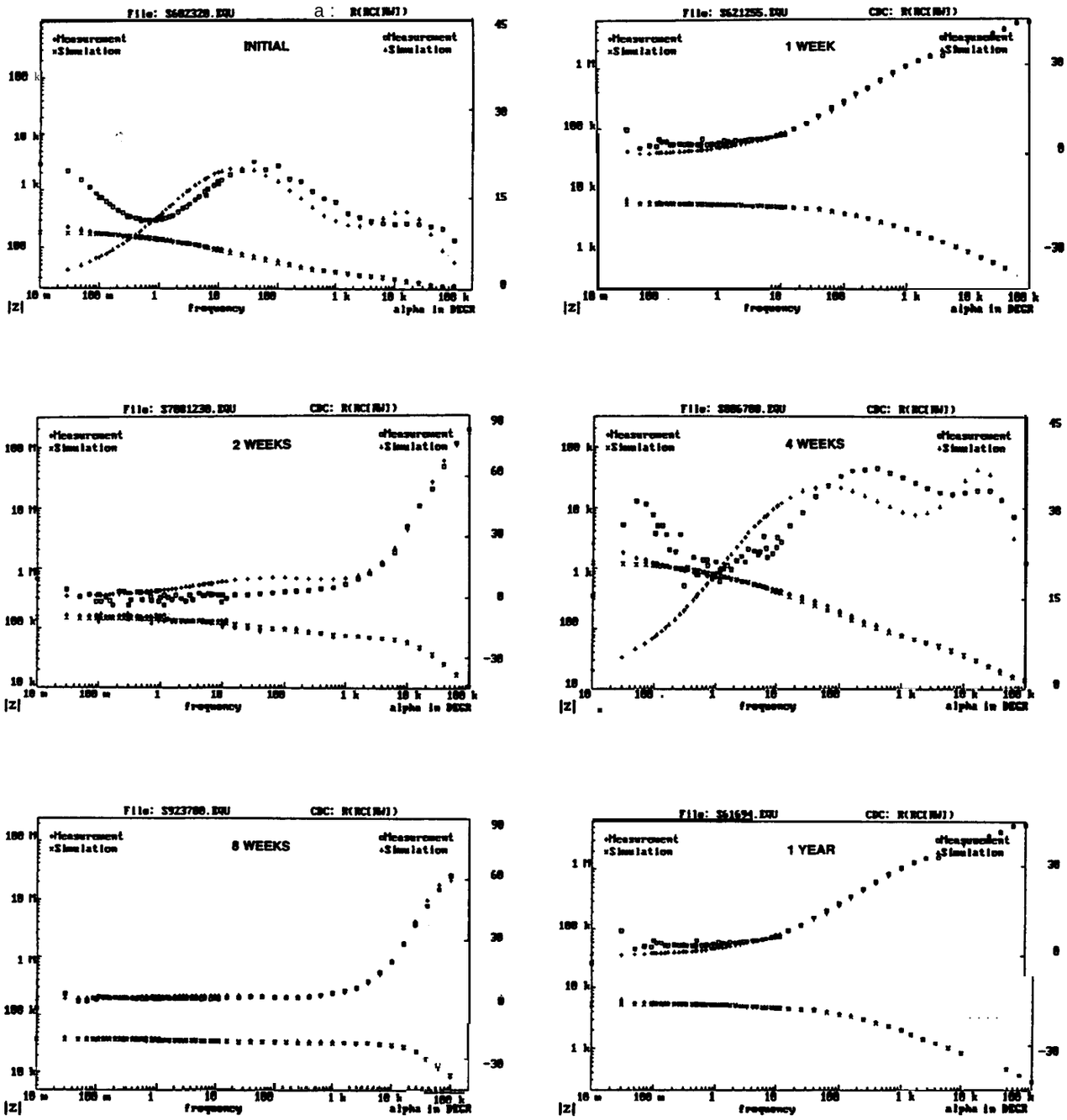

FIGUREA-37. BODEPLOTSOFKOPPERS701

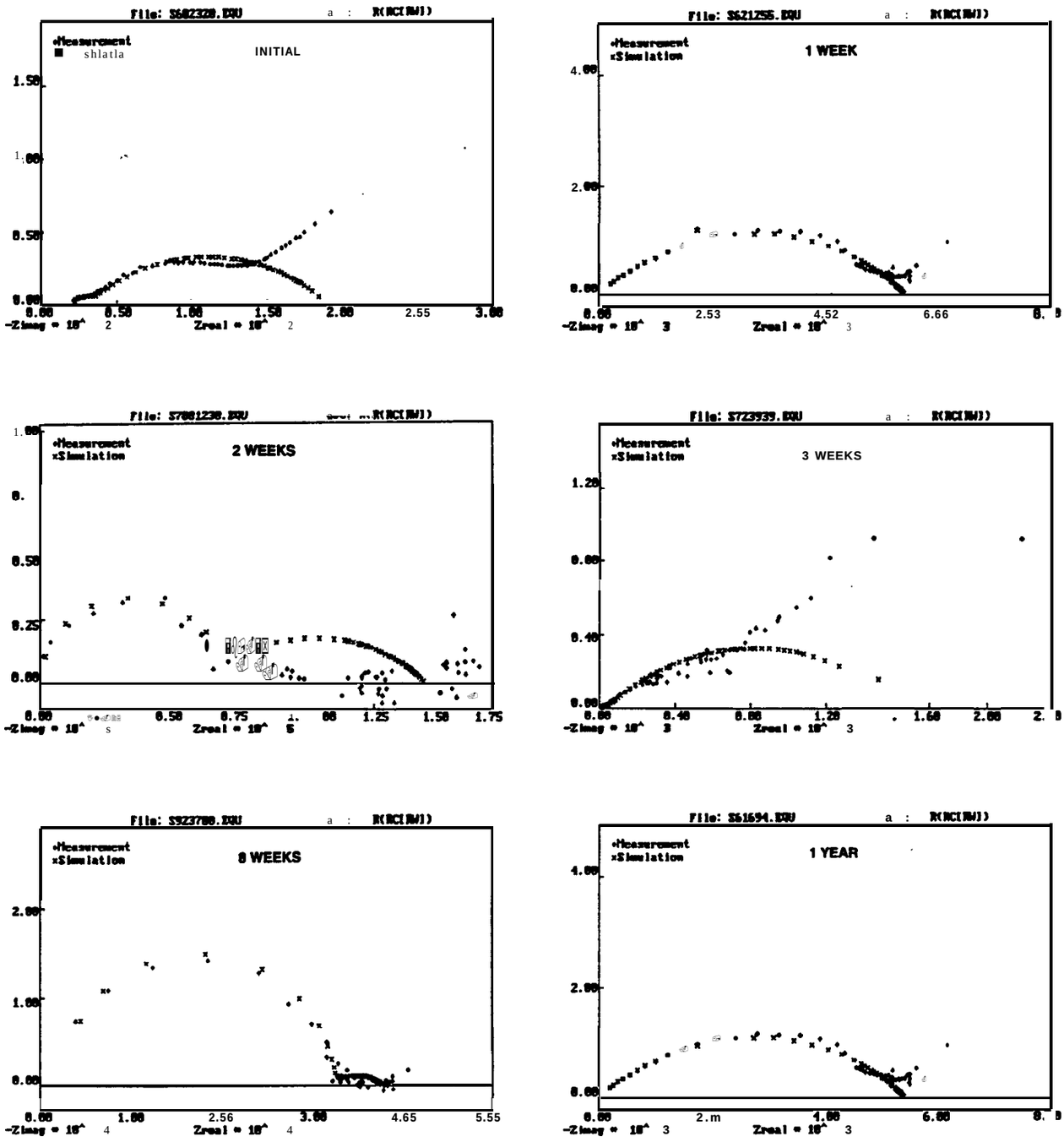

FIGURE A-38. NYQUIST PLOTS OF KOPPERS 701

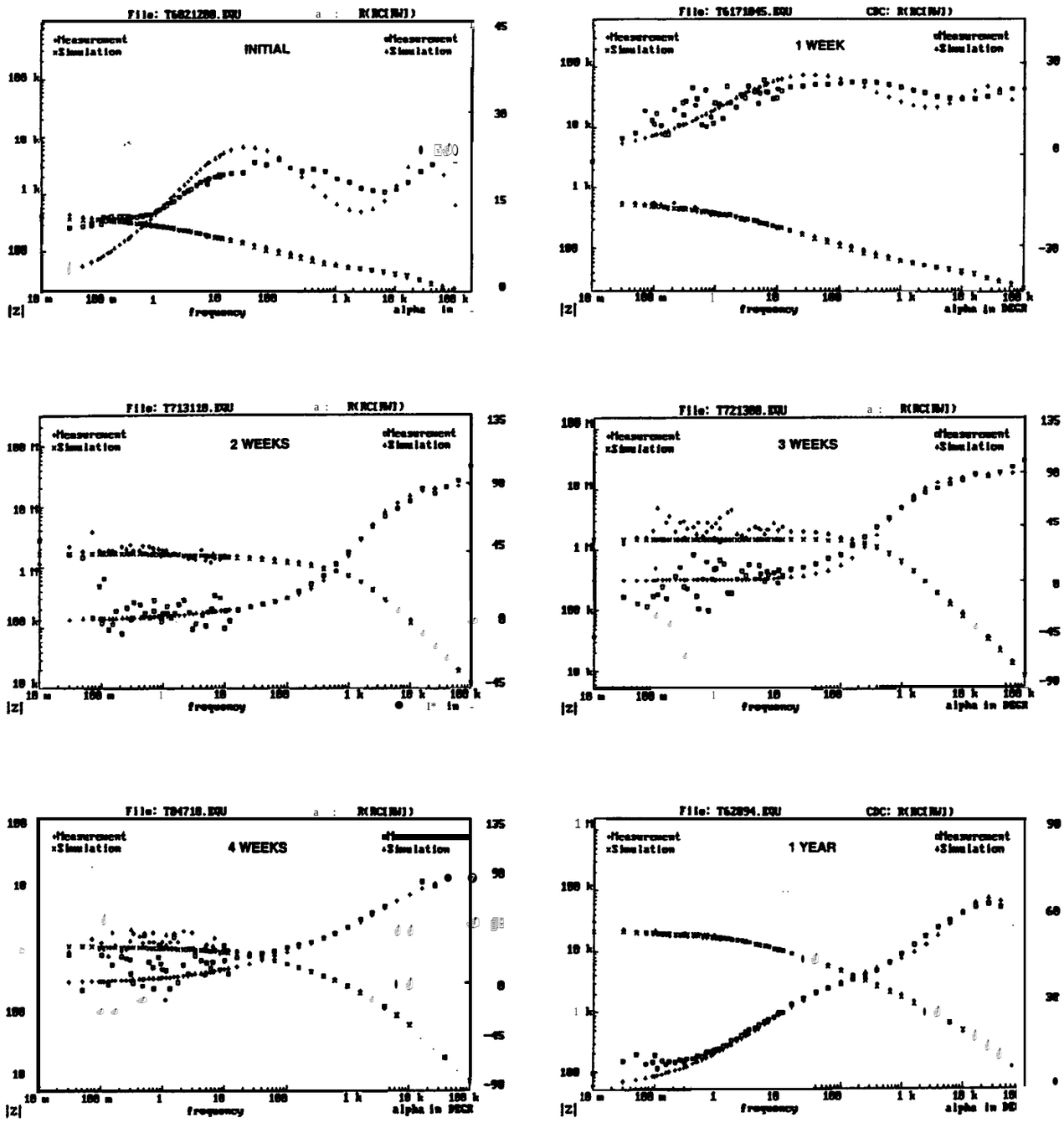

FIGURE A-39. BODEPLOTSOFSUBOXGALVANOXV

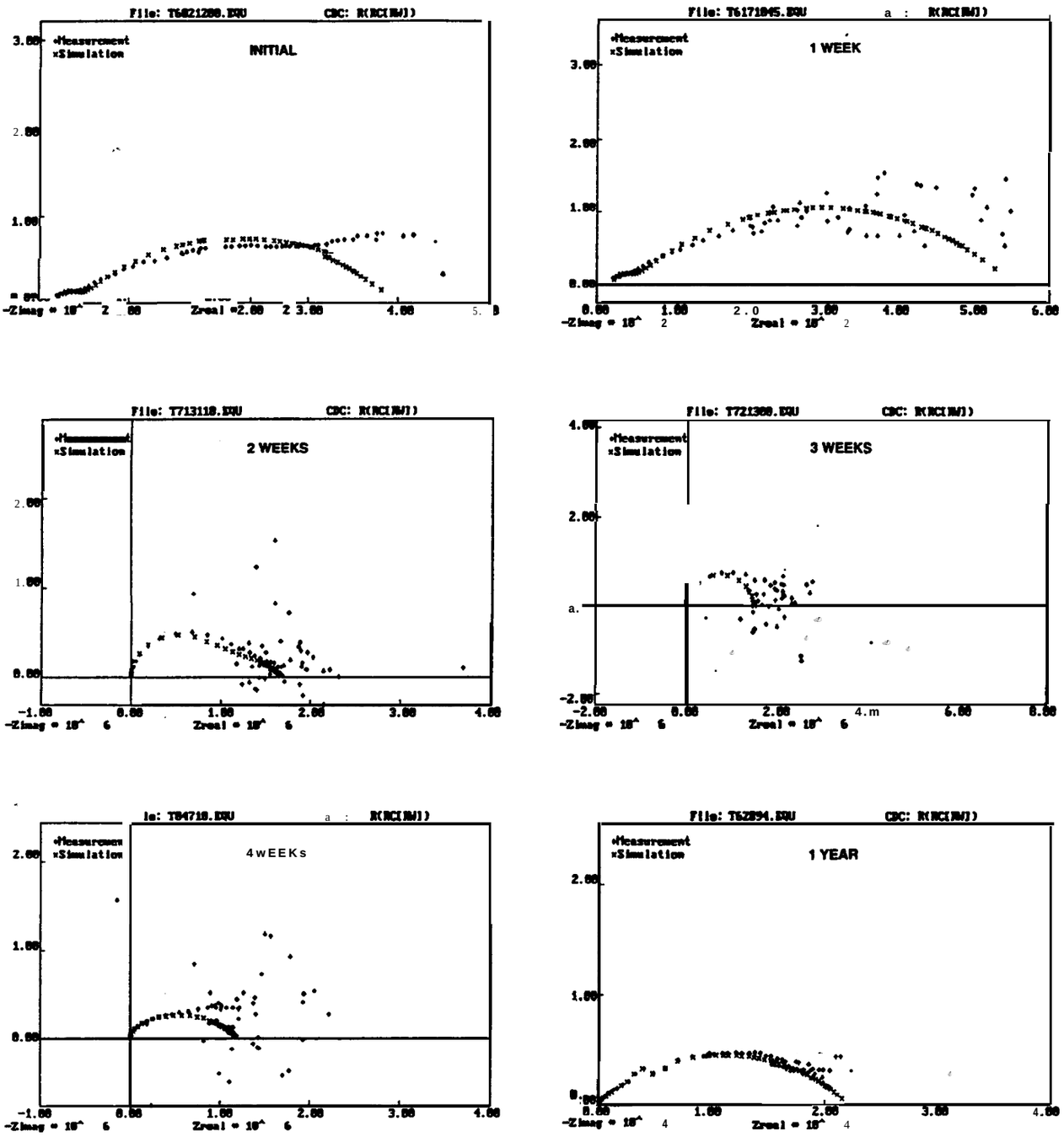

FIGURE A-40. NYQUISTPLOTSOFSUBOXGALVANOXV

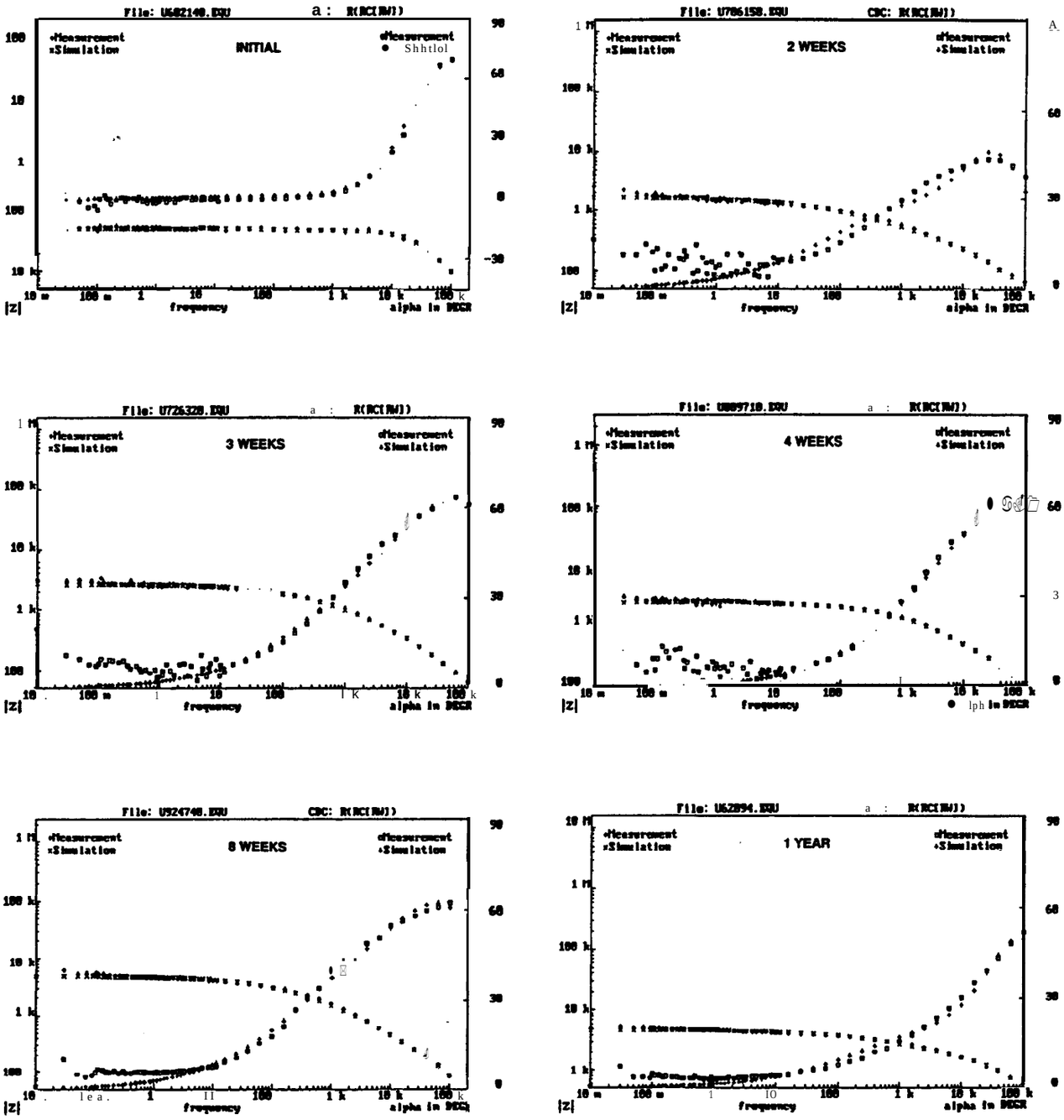

FIGURE A-41. BODE PLOTS OF TNEMEC 903-75

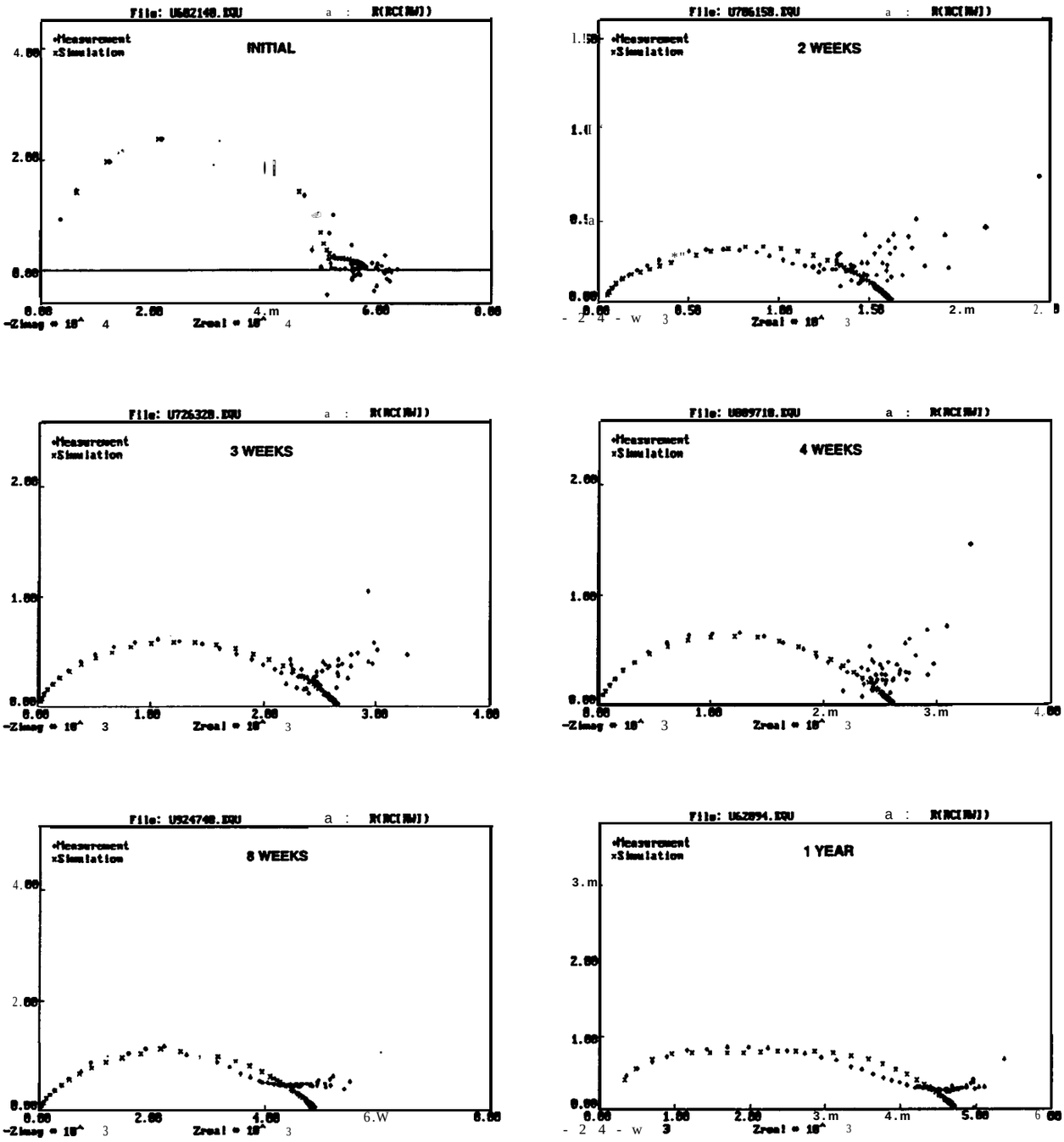

FIGUREA-42. NYQUIST PLOTS OF 90E-75

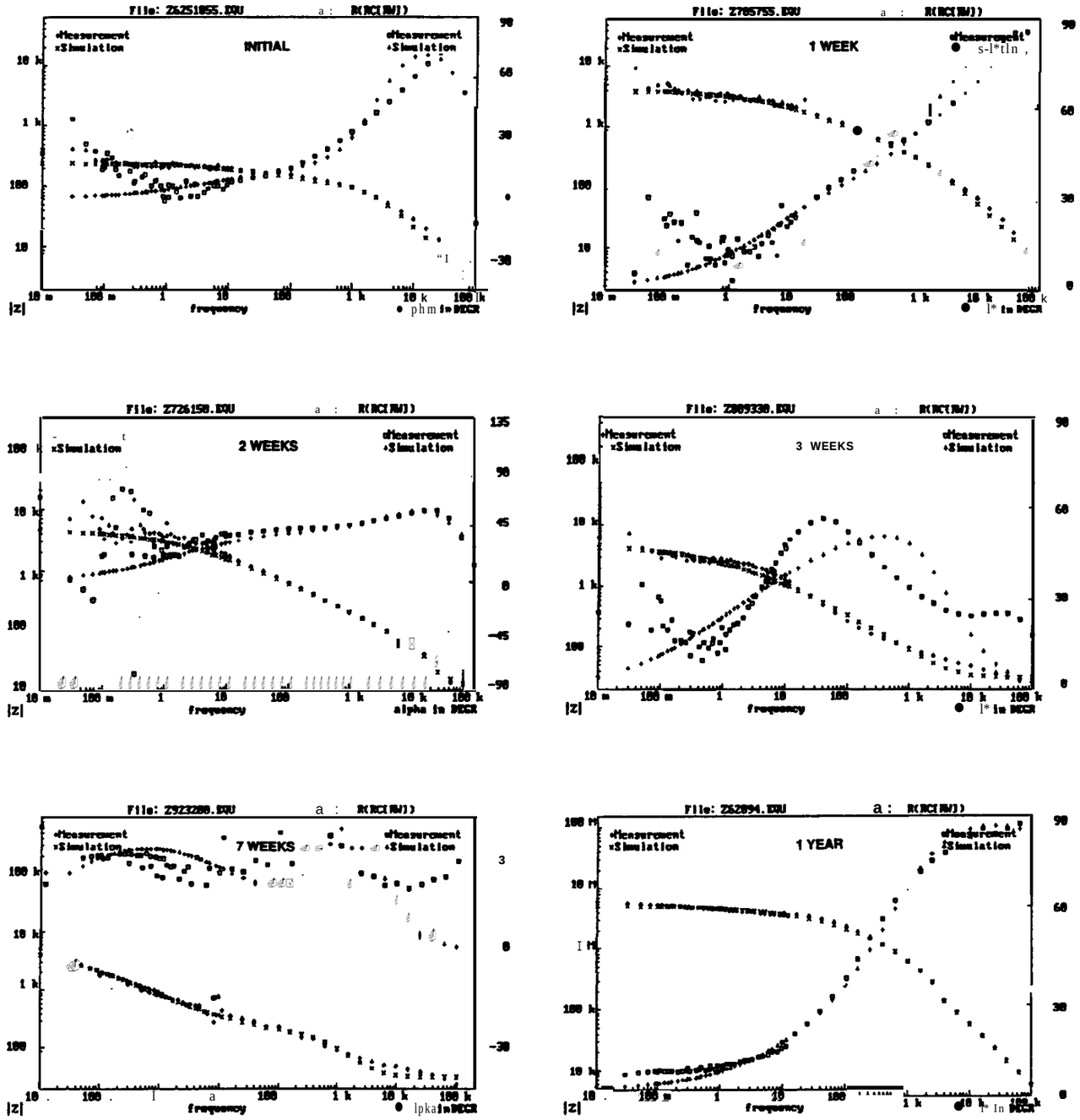

FIGURE A-43. BODE PLOTS OF GALVANIZED STEEL

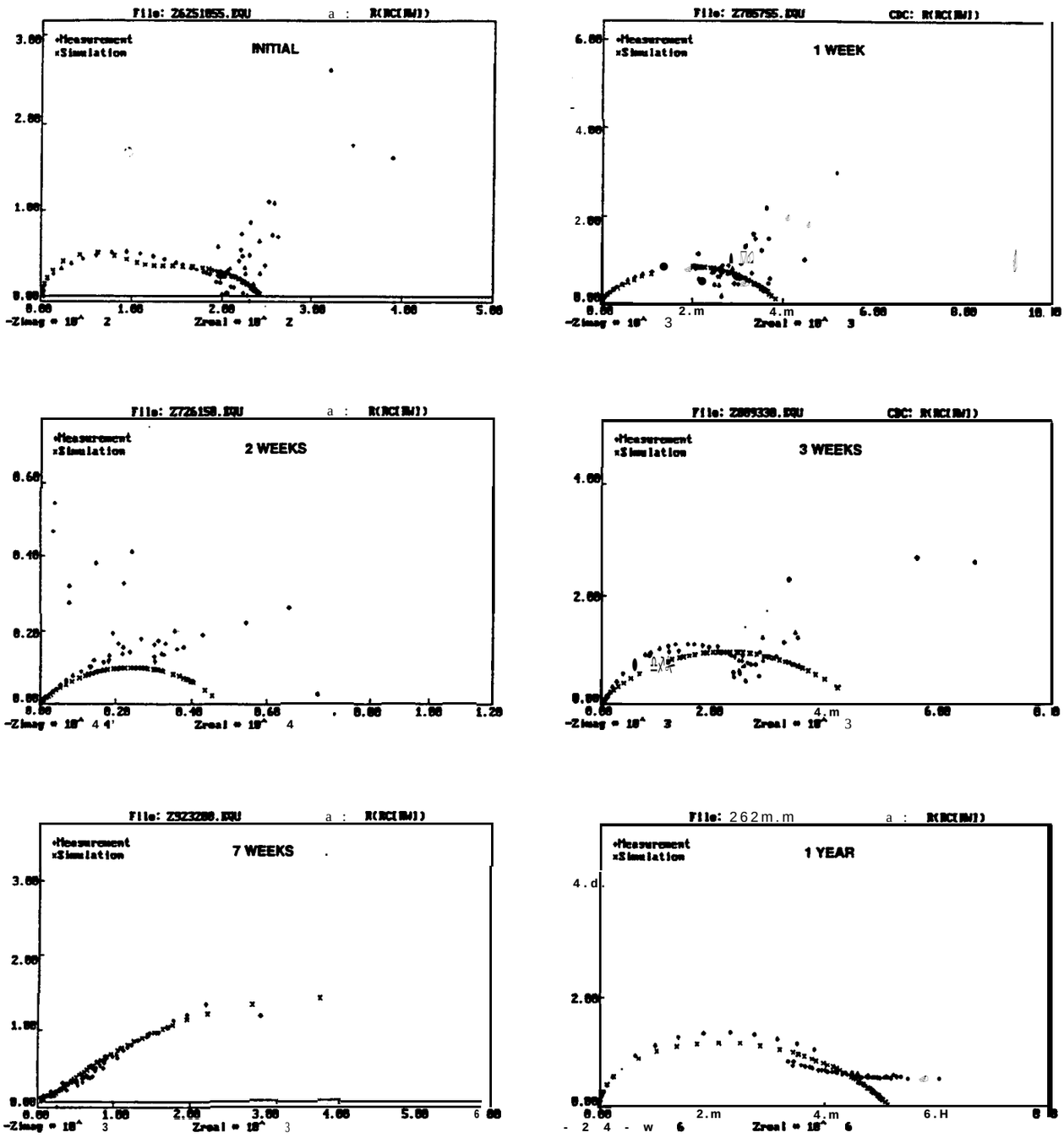

FIGURE A-44. NYQUIST PLOTS OF GALVANIZED STEEL